iScience

CellPress
OPEN ACCESS

Article

Ubiquitin-specific peptidase 22 controls integrin-dependent cancer cell stemness and metastasis

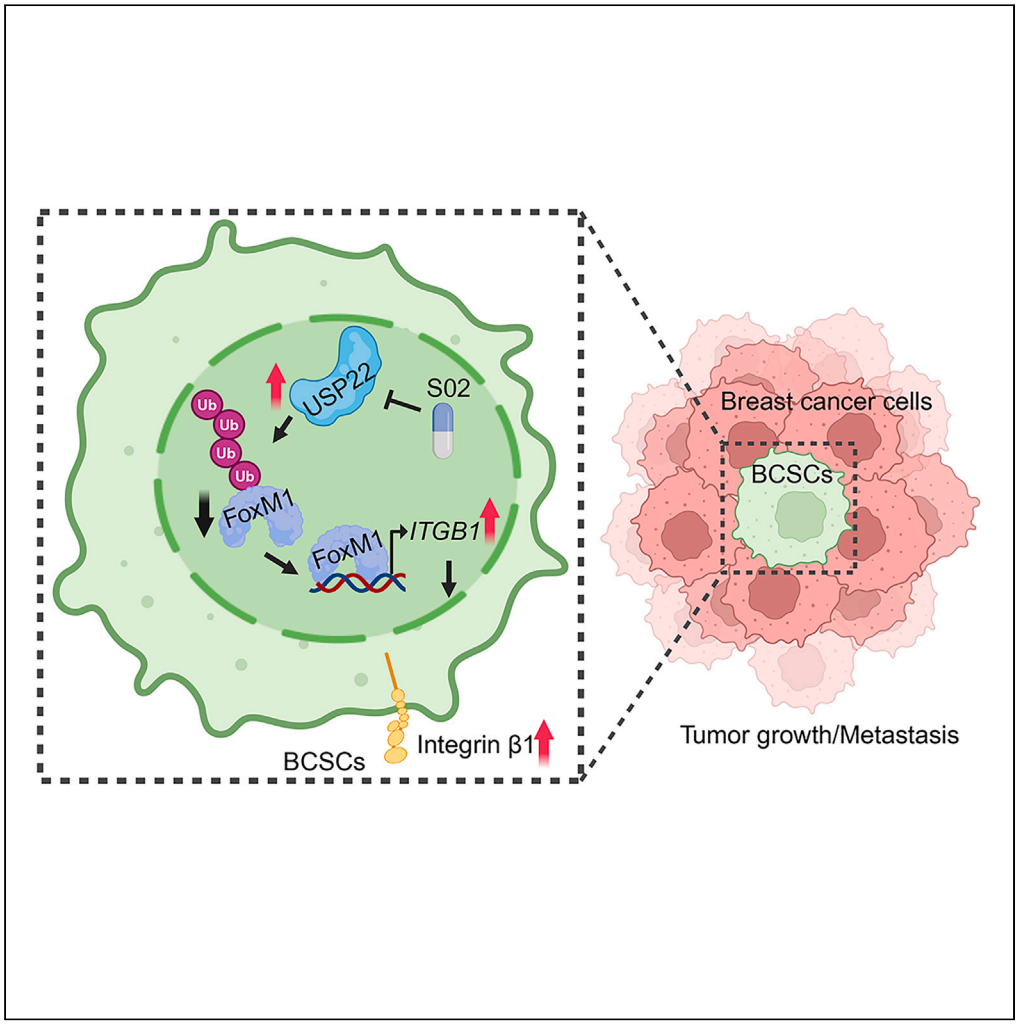

Kun Liu, Qiong Gao, Yuzhi Jia, ..., Bin Zhang, Huiping Liu, Deyu Fang

fangd@northwestern.edu

Highlights

USP22 maintains breast cancer stemness and promotes metastasis

FoxM1/integrin β1 is essential for USP22 mediated metastasis in breast cancer

USP22/FoxM1/integrin β1 is highly expressed in breast cancer

USP22i-S02 offers new option for breast cancer treatment

Liu et al., iScience *27*, 110592
September 20, 2024
https://doi.org/10.1016/j.isci.2024.110592

iScience

CellPress
OPEN ACCESS

Article

Ubiquitin-specific peptidase 22 controls integrin-dependent cancer cell stemness and metastasis

Kun Liu,[1,5] Qiong Gao,[1,2,5] Yuzhi Jia,[3] Juncheng Wei,[1] Shuvam Mohan Chaudhuri,[1] Shengnan Wang,[1] Amy Tang,[1] Nikita Lavanya Mani,[1] Radhika Iyer,[1] Yang Cheng,[1] Beixue Gao,[1] Weiyuan Lu,[1] Zhaolin Sun,[2] Bin Zhang,[3] Huiping Liu,[4] and Deyu Fang[1,6,*]

SUMMARY

Integrins play critical roles in connecting the extracellular matrix and actin. While the upregulation of integrins is thought to promote cancer stemness and metastasis, the mechanisms underlying their upregulation in cancer stem cells (CSCs) remain poorly understood. Herein, we show that USP22 is essential in maintaining breast cancer cell stemness by promoting the transcription of integrin β1 (*ITGB1*). Both genetic and pharmacological inhibition of USP22 largely impaired breast CSCs self-renewal and prevented their metastasis. Reconstitution of integrin β1 partially rescued USP22-null breast cancer metastasis. USP22 functions as a bona fide deubiquitinase to protect the proteasomal degradation of the forkhead box M1 (FoxM1), a transcription factor for tumoral *ITGB1* gene transcription. Immunohistochemistry staining detected a positive correlation among USP22, FoxM1, and integrin β1 in human breast cancers. Collectively, our study identifies the USP22-FoxM1-integrin β1 signaling axis as critical for cancer stemness and offers a potential target for antitumor therapy.

INTRODUCTION

Despite recent therapeutic advances in tumor treatment, metastasis to the nearby or distal organs remains the main cause of cancer-related death.[1] It has been proposed that only a small portion of primary tumor cells, termed cancer stem cells (CSCs), are responsible for metastasis.[2] CSCs are a small population in the tumor that is self-renewable, preferentially aggressive, and responsible for cancer initiation, metastasis, and recurrence.[3] Breast cancer stem cells (BCSCs), for example, have antioxidative, tumor sphere formation, and chemoresistance properties. Based on cell surface marker expression, BCSCs are CD44(+)/CD24(−/low) tumorigenic cells that initiate tumors in xenografts.[4] CD44 is a cell surface glycoprotein and stemness marker in BCSCs. CD44 binds to hyaluronic acid and mediates the interactions between cell-cell and cell-matrix proteins, such as matrix metalloprotease and osteopontin.[5] We have recently discovered that CD44 homophilic interactions and subsequent CD44-PAK2 interactions mediate tumor cluster aggregation and metastasis.[6] While some progress has been made to characterize CSCs over the last decade, the cellular and molecular mechanisms underlying how CSCs are generated and how their self-renewal is maintained remain largely unknown.

The ubiquitin-specific peptidase 22 (USP22) was initially identified as one of the 11 genes in cancer-related death signatures referred to as the polycomb/CSCs signature group.[7] Further survey of gene expression has shown that the elevated expression of USP22 correlates with poor prognosis in a variety of human tumors including the invasive breast cancer.[8,9] At the molecular level, we and others have recently demonstrated that USP22 functions as an oncogene by inhibiting cell apoptosis and promoting cell cycle progression through targeting cyclins, c-MYC, BMI-1, TRF1, and SIRT1, which controls p53 expression.[10–15] USP22 promotes chemotherapeutic resistance by inhibiting Bax-mediated apoptosis, improving HSP90 function, inhibiting estrogen receptor α degradation, and driving epidermal growth factor receptor recirculation.[16] Genetic USP22 suppression inhibits cancer cell growth and induces apoptosis.[10,13] USP22 has been speculated to act as a critical CSCs gene,[17] however, the molecular pathways underlying if and how USP22 maintain cancer cell stemness and control CSCs self-renewal remain to be fully defined.

[1]Department of Pathology, Robert H. Lurie Comprehensive Cancer Center, Northwestern University Feinberg School of Medicine, Chicago, IL 60611, USA
[2]College of Basic Medical Sciences, Dalian Medical University, Dalian 116044, P.R. China
[3]Department of Medicine, Hematology/Oncology Division, Robert H. Lurie Comprehensive Cancer Center, Northwestern University Feinberg School of Medicine, Chicago, IL 60611, USA
[4]Department of Pharmacology, Robert H. Lurie Comprehensive Cancer Center, Northwestern University Feinberg School of Medicine, Chicago, IL 60611, USA
[5]These authors contributed equally
[6]Lead contact
*Correspondence: fangd@northwestern.edu
https://doi.org/10.1016/j.isci.2024.110592

In this study, we present evidence that USP22 is highly expressed in BCSCs and is required for both breast cancer initiation and metastasis. Both genetic and pharmacological USP22 inhibition largely reduced the BCSCs pool through downregulating integrin β1, also known as CD29, a cell surface glycoprotein that is critical in almost every step of cancer progression, including cancer initiation, proliferation, local invasion, and metastatic colonization of the new tissue.[18,19] Interestingly, integrin β1 has been used as a biomarker for isolating BCSCs.[20] Indeed, reconstitution of integrin β1 expression fully rescued the BCSCs pool impaired by USP22 deficiency. At the molecular level, we identified the *ITGB1* transcription factor FoxM1 as a *de novo* substrate of the USP22 deubiquitinase. Therefore, USP22 controls BCSCs self-renewal through protecting FoxM1 from ubiquitination-mediated proteasomal degradation to enhance *ITGB1* transcription. Our study defines the USP22-FoxM-integrin β1 axis as a previously unappreciated pathway in breast cancer initiation and metastasis that can be therapeutically targeted to antagonize invasive breast cancers.

RESULTS

USP22 is required for the tumorigenicity of BCSCs

USP22 has been suggested as a CSC gene or death-from cancer signature gene and high USP22 expression often predicts poor clinical outcomes of cancer patients.[7] However, its role in maintaining CSCs stemness remains to be defined. We sorted $CD24^{-}CD44^{+}$ breast CSCs from patient-derived Luc2-eGFP (L2G)-labeled breast triple-negative (TN1) cancer cells[6] as well as from murine breast cancer 4T1 cells (Figure S1A) and found a higher USP22 expression in breast CSCs compared to $CD24^{+}CD44^{-}$ non-BCSCs by western blotting (Figures 1A and 1B; Figure S1B). To decipher the functional consequences of USP22 loss in initiating and/or maintaining breast cancer cell stemness, we generated USP22 targeted deletion in mouse 4T1 and human breast cancer-derived $L2G^{+}$ TN1 cells using CRISPR-Cas9. Complete deletion of USP22 was verified by immunoblot analysis (Figures 1C and S1C). Importantly, silencing USP22 reduced the $CD24^{-}CD44^{+}$ breast CSCs population in $L2G^{+}$ TN1 and 4T1 cells (Figures 1D, S1D, and S1E), indicating that USP22 is important for breast CSCs self-renewal. We then utilized a well-established tumor sphere formation assay[21,22] to evaluate the role of USP22 in breast CSCs self-renewal. Indeed, the tumor sphere formation from both patient derived $L2G^{+}$ TN1 and mouse 4T1 breast cancer cells was largely impaired by USP22 CRISPR deletion, which was further confirmed by an *in vitro* extreme limiting dilution assay (Figures 1E–1G and S1F–S1H). Consistently, USP22 inhibition in 4T1 cells resulted in a substantial reduction of colony formation ability (Figures S1I and S1J). Next, we expanded our findings by evaluating the CSCs population in MC38 and LLC1 USP22-deficient and control cells. The loss of USP22 exhibited a smaller CSCs population compared with control cells (Figures S1K and S1L). In line with these results, USP22 depletion led to impaired tumor sphere formation ability in MC38 and LLC1 cells as evidenced by the reduced tumor spheres number in USP22-deficient cells compared with control cells (Figures S1M and S1N). Therefore, these results support the data that USP22 is required to maintain an optimal CSCs population *in vitro*, possibly by controlling CSCs self-renewal.

CSCs are a critical small population of cancer cells with potent capability for tumor initiation. To evaluate the functional sequences of USP22 in promoting tumor initiation *in vivo*, we orthotopically injected 10^2, 10^3, and 10^4 USP22 knockout or control 4T1 breast cancer cells into BALB/c mice. Surprisingly, in contrast to the fact that five out of eight mice implanted with 10^2 WT 4T1 cells developed cancer three months after implantation, none of the eight mice receiving USP22-deficient 4T1 cells developed breast cancer. Even when a higher number of 4T1 cells, 10^3 and 10^4, were orthotopically injected, USP22 deletion inhibited the development of syngeneic tumors (Figures 1H and 1I), indicating that USP22 is critical for *in vivo* tumor initiation. Cancer metastases, per prevailing theory, are predominantly initiated by rare cancer cells that bear stem cells properties.[23,24] We then investigated whether USP22 exerted a driving role in breast cancer metastasis by intravenous injection of 4T1 USP22-null or its control WT cells into BALB/c mice. As expected, USP22 deletion inhibited 4T1 cancer colonization of the lung by reducing more than 60% of tumor nodules with further reduction in metastatic foci size (Figures 1J–1L). Immunohistochemistry (IHC) staining confirmed the deletion of USP22 and detected a significant decrease in the expression levels of stem cell marker CD44 in lung metastasis (Figures 1M and 1N). Consequently, USP22 ablation significantly improved the overall survival of mice with 4T1 lung metastasis (Figure 1O). Collectively, our results revealed that USP22 plays an important role in BCSCs maintenance and is therefore critical for breast cancer initiation and metastasis.

USP22 promotes BCSCs self-renewal through upregulating *ITGB1* expression

Integrin family members are known as key regulators of cancer cell stemness, epithelial-mesenchymal transformation, and extracellular matrix to initiate the metastatic program for multiple cancer types including breast cancer.[19,25] Therefore, we investigated the expression patterns of USP22 and integrin family members in breast cancer cell lines sourced from the Cancer Cell Line Encyclopedia (CCLE). Our analysis revealed a positive correlation between USP22 expression and *ITGB1*, *ITGB3*, or *ITGAE*, but not other integrin family members (Figures 2A and S2A), implying that USP22 may contribute to breast cancer progression by modulating integrin family members. Subsequently, we assessed the transcript levels of *ITGB1*, *ITGB3*, or *ITGAE* in USP22-depleted and control cells. Our findings demonstrated that USP22 depletion resulted in a more than 70% reduction in *ITGB1* transcripts, while *ITGB3* or *ITGAE* levels remained unaffected (Figure 2B), highlighting USP22 as a novel regulator of *ITGB1*. Further flow cytometric analysis of integrin family members in WT and USP22-null breast cancer cells revealed a significant decrease in integrin β1 expression upon USP22 inhibition in both mouse 4T1 and patient-derived $L2G^{+}$ TN1 cells (Figures 2C and 2D). In addition to integrin β1, USP22 deletion led to a slight cell surface reduction of several additional integrin family members including integrin α1-6 and integrin β2-3 and β5-7 but not β4, β8, and α7-8 expression determined by flow cytometry (Figure S2B). In contrast, integrin β6 expression is slightly increased in USP22-null breast cancer cells (Figure S2B). Moreover, immune blotting confirmed the reduction in integrin β1 expression by USP22 inhibition (Figure 2E). The optimal *ITGB1* promoter region was amplified and inserted into a firefly luciferase reporter. As expected,

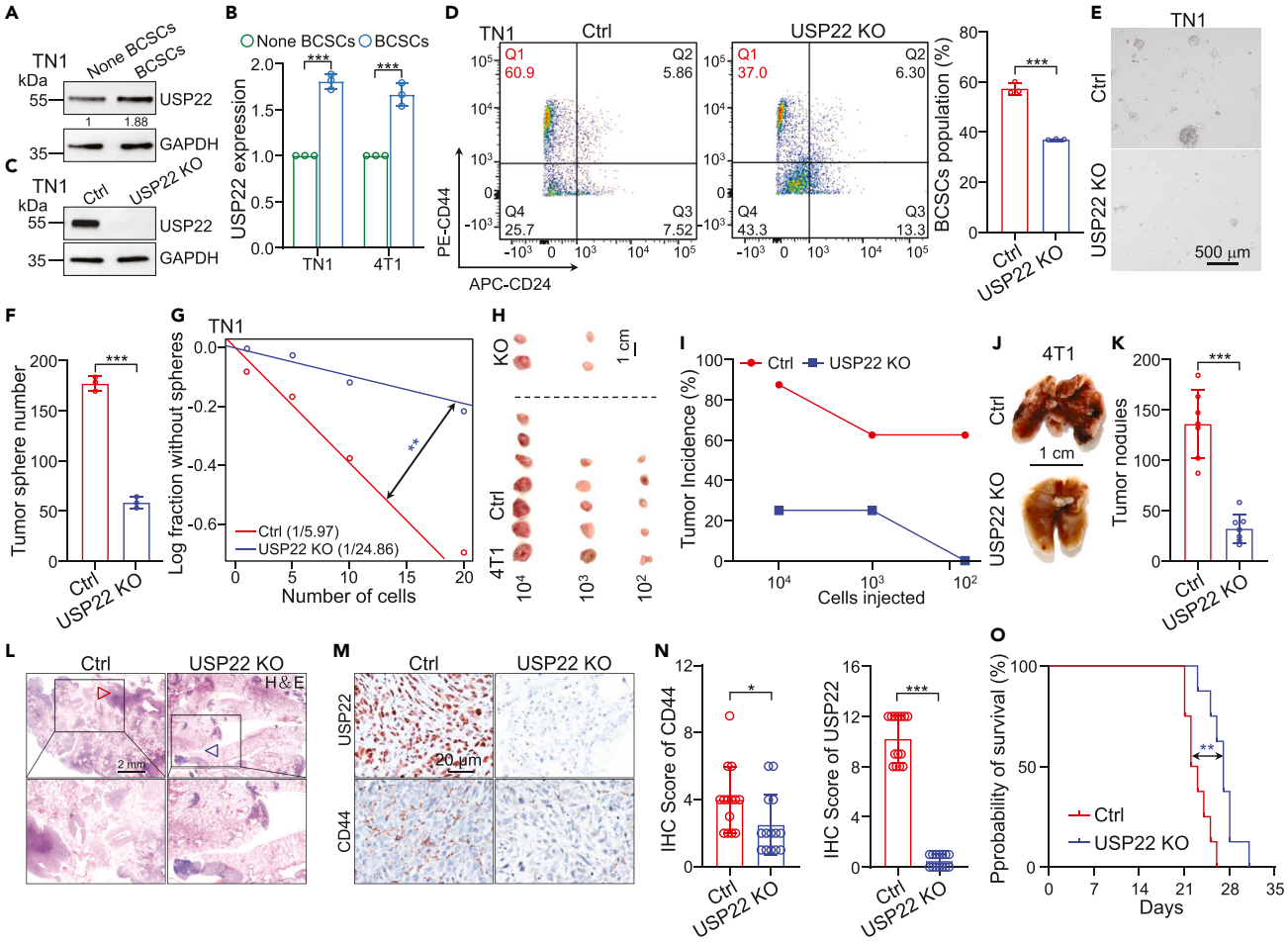

Figure 1. USP22 is required for BCSCs tumorigenicity

(A) Immunoblot assessment of USP22 across matched pairs of tumor sphere-enriched BCSCs and non-BCSCs of TN1 cells. Band intensities of USP22 were quantified and the results are expressed as USP22/GAPDH levels relative to control cells.

(B) Quantification showing that USP22 was highly expressed in BCSCs than in non-BCSCs.

(C) TN1 cells were transduced with single guide RNA (sgRNA) targeting USP22 or a scrambled control sgRNA, and knockout efficiency of USP22 was determined by immunoblot analyses.

(D) USP22 ablation decreases BCSCs ($CD44^{+}CD24^{-}$) population in TN1 cells as determined by flow cytometry. Representative FACS data are shown. Quantification data showing that BCSCs population in USP22-deficent cells was decreased than control cells.

(E) Tumor sphere formation ability was evaluated in TN1 cells expressing either control or USP22 sgRNA, and the representative images of each group are shown. Scale bar, 500 μm.

(F) Silencing USP22 markedly impairs TN1 cells tumor sphere formation ability.

(G) The frequencies of tumor sphere formation of TN1 USP22 ablation or control cells determined by *in vitro* extreme dilution analysis. The significance of the difference between the indicated groups was evaluated by χ^2 test. $n = 10$. The frequency of CSCs was shown.

(H) Images of tumors from mice orthotopically implanted with indicated different gradients of 4T1 USP22 ablation or control cells. $n = 8$.

(I) Quantification showing that USP22 ablation impairs breast cancer initiation.

(J) Representative images of lung from mice intravenously injected with 4T1 cells expressing either control or USP22 sgRNA. Scale bar, 1 cm

(K) The mice were sacrificed after 20 days injection of indicated 4T1 cells. The numbers of metastatic nodules in the lung were significantly decreased in mice injected with 4T1 USP22 knockout cells compared with those injected with 4T1 control cells.

(L) The hematoxylin and eosin (H&E) staining show metastatic tumor. Scale bar, 2 mm.

(M) Immunohistochemical staining using anti-USP22 or CD44 antibodies were performed on metastatic nodules. Representative images of each group are shown. Scale bar, 20 μm.

(N) Quantification showing that USP22 knockout induced the decrease of CD44 positive cells.

(O) Kaplan-Meier survival curve of mice intravenously injected with 4T1 cells lacking or expressing USP22 sgRNA. Quantifications showing that injecting USP22 ablation cells extended mice survival relative to control group. The significance of the difference between the indicated groups was evaluated by log-rank test. $n = 8$. The error bars show the mean ± SD. The significances of differences between groups were determined by two-tailed Student's t test. *, *** indicates $p < 0.05$, $p < 0.001$, respectively.

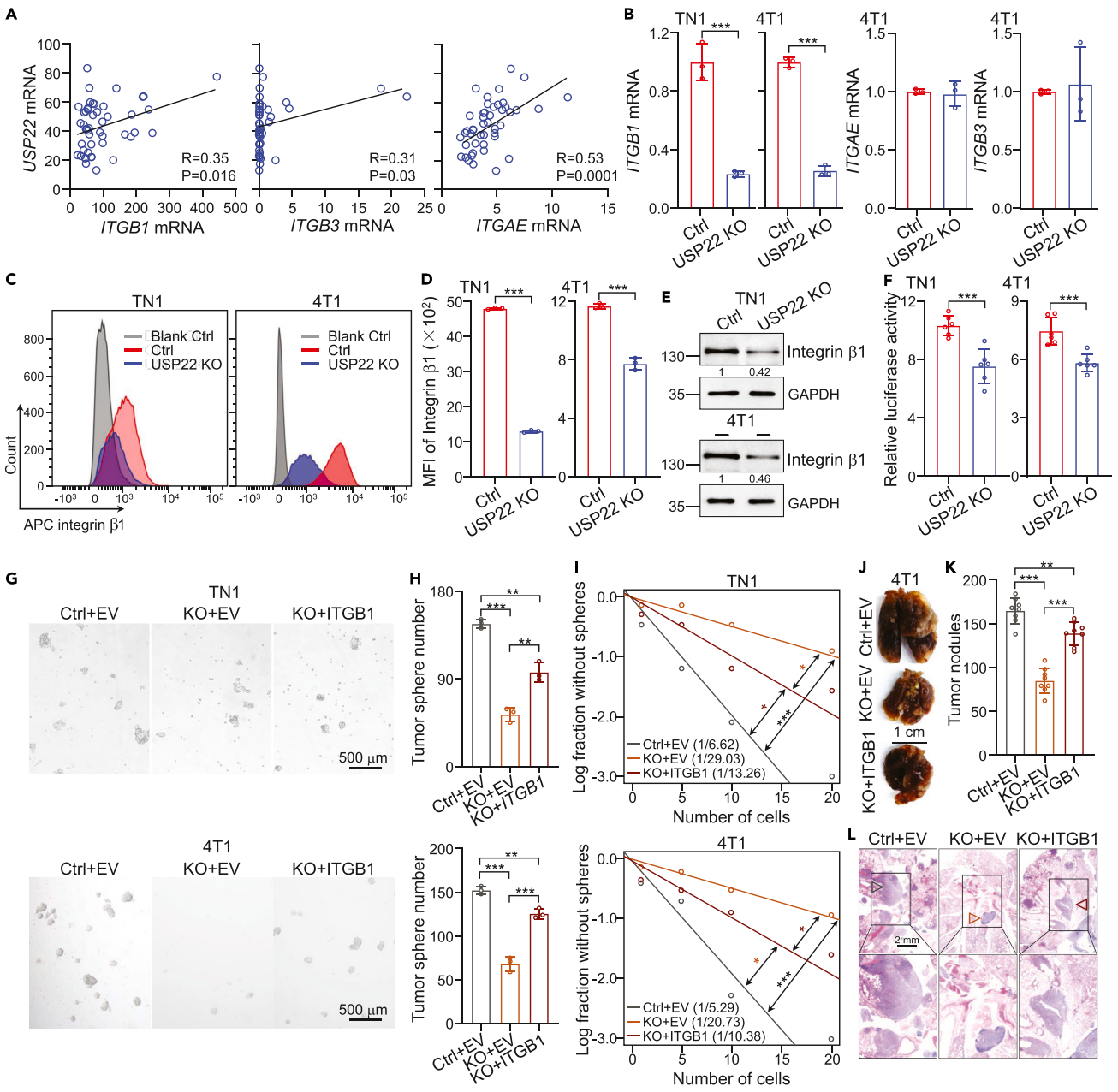

Figure 2. Depleting USP22 prohibits integrin β1 expression

(A) Correlation of the transcripts of USP22 and *ITGB1*, *ITGB3*, and *ITGAE* in breast cancer cell lines from CCLE database.

(B) The mRNA expression of *ITGB1* (gene encoding for integrin β1), *ITGB3* (gene encoding for integrin β3), and *ITGAE* (gene encoding for integrin αE) in USP22 ablation or control cells was determined by real-time PCR. β-actin was used as an internal control.

(C) Integrin β1 level was decreased in USP22 ablation cells as determined by flow cytometry. Representative FACS data are shown.

(D) Mean fluorescence intensity (MFI) of integrin β1 level in TN1 and 4T1 USP22-deficent or control cells was quantified.

(E) Indicated protein expression in TN1 and 4T1 cells expressing either control or USP22 sgRNA were determined by immunoblot analysis. Band intensities of integrin β1 were quantified, and the results are expressed as integrin β1/GAPDH levels relative to control cells.

(F) Luciferase activity of vector containing *ITGB1* promoter in TN1 and 4T1 cells with or without USP22 depletion.

(G and H) The representative images (F) and number (G) of tumor sphere formed from TN1 and 4T1 cells transduced with integrin β1 in the setting of USP22 depletion. Scale bar, 500 μm.

Figure 2. *Continued*

(I) The frequencies of tumor sphere formation of indicated cells. Quantifications showing that introduction of integrin β1 restores tumor sphere formation frequency caused by USP22 depletion evaluated by *in vitro* extreme limiting dilution analysis. The significance of the difference between the indicated groups was evaluated by χ^2 test. $n = 10$. The frequency of CSCs was shown.

(J) Representative images of lung from mice intravenously injected with indicated cells. Scale bar, 1 cm.

(K) The numbers of metastatic nodules in the lung from mice intravenously injected with indicated cells.

(L) H&E staining of lung metastasis of indicated group. Scale bar, 2 mm. The error bars show the mean ± SD. The significances of differences between groups were determined by two-tailed Student's t test. **, *** indicates $p < 0.01$, $p < 0.001$, respectively.

a significant reduction in ITGB1 luciferase activity was detected in transiently transfected USP22 KO TN1 and 4T1 comparing to that in control WT cells, suggesting that USP22 is involved in transcriptionally regulating *ITGB1* (Figure 2F).

We then focused on studying the functional consequences of USP22-mediated integrin β1 upregulation and assessed whether USP22 maintains BCSCs self-renewal and promotes breast cancer metastasis through integrin β1 upregulation by ectopic reconstitution of *ITGB1* in USP22 knockout cells (Figures S2C–S2E). Indeed, ectopic *ITGB1* expression partially rescued tumor sphere formation in both mouse 4T1 and patient-derived L2G$^+$ TN1 USP22-deficient breast cancer cells (Figures 2G–2I). Consequently, expression of integrin β1 largely restored 4T1 breast cancer lung metastasis of USP22-null cells as documented by analyzing both lung tumor nodule numbers and the metastatic foci size (Figures 2J–2L). Collectively, these results demonstrate that USP22 enhances BCSCs tumorigenicity in part through integrin β1 upregulation.

USP22 functions as a *de novo* FoxM1-specific deubiquitinase in breast cancer cells

The fact that USP22 deletion reduced *ITGB1* mRNA expression suggests that USP22 regulates integrin β1 expression at the transcriptional level. Indeed, western blot analysis revealed a significant reduction in the protein expression of FoxM1, a critical transcription factor for *ITGB1* expression,[26] in USP22 loss breast cancer cells (Figure 3A). In contrast, USP22 ablation did not alter *FoxM1* mRNA levels (Figure 3B). Together with the fact that USP22 is a deubiquitinase, these results imply that the USP22 exerts its regulatory function on FoxM1 protein expression at the post-transcriptional level. Indeed, treatment of USP22-null cells with the proteasome inhibitor MG132 largely restored FoxM1 expression to a level comparable to that of WT breast cancer cells (Figure 3A). By contrast, treatment with NH_4Cl, an inhibitor of endosome-lysosome degradation pathway, fails to protect FoxM1 from degradation (Figure S3A), suggesting that USP22 promotes FoxM1 expression by inhibiting its proteasomal degradation.

As a deubiquitinase, USP22 exerts its biological function largely through protecting its downstream substrates from ubiquitination-mediated degradation.[27] Accordingly, we speculated that USP22 could be a deubiquitinase of FoxM1. Indeed, USP22 interaction with FoxM1 was detected in HEK-293T cells transiently transfected with Myc-USP22 and Flag-FoxM1 but not in control cells transfected with Flag-FoxM1 or Myc-USP22 alone (Figure 3C). The endogenous interaction between USP22 and FoxM1 was further validated in patient-derived breast cancer L2G$^+$ TN1 and 4T1 cells (Figures 3D and S3B). USP22 protein carries an N-terminal zinc finger and C-terminal U19 peptidase catalytic domain (Figure 3E). Truncated mutation analysis revealed that the zinc finger-containing N-terminus is sufficient for USP22 interaction with FoxM1, while the C-terminus ubiquitin-specific peptidase domain is not involved in mediating its FoxM1 interaction (Figure 3F). These results indicate that FoxM1 physically interacts with USP22 in breast cancer cells.

The N-terminal zinc finger of USP22 is required for its interaction between with FoxM1 is required, since mutation of cysteines 61 and 63 completely disrupted their interaction (Figure 3G). In concordance with this conclusion, USP22 overexpression prolonged FoxM1 half-life as measured by cycloheximide pulse-chase analysis (Figures 3H and 3I). In line with these results, neither USP22 C185A nor C61/63A mutant sustained FoxM1 stability (Figures 3H and 3I). In line with this, the half-life of FoxM1 was decreased in the presence of USP22 loss (Figures 3J and 3K). Subsequently, re-expression of WT USP22 but not its mutants restored integrin β1 protein and transcript level in USP22-null breast cancer cells (Figures 3L and S3C). Additionally, mutation of cysteines 61 and 63 totally abolished USP22 activity in suppressing FoxM1 ubiquitination (Figure 3M). As expected, expression of the catalytically inactive USP22, through C185A mutation, failed to inhibit FoxM1 ubiquitination despite not altering its interaction with FoxM1 (Figures 3G and 3M). These results indicate that USP22 is a bona fide FoxM1-specific deubiquitinase in breast cancer cells. A ubiquitin-specific peptidase exerts its function through inhibiting ubiquitination of its interacting proteins.[28] Thus, we determined the effect of USP22 on FoxM1 ubiquitination. Higher molecular weight bands were detected in FoxM1 immunoprecipitants, indicating FoxM1 is ubiquitinated possibly by its endogenous E3 ubiquitin ligases such as FBWX7.[29] Importantly, transient USP22 expression largely diminished FoxM1 ubiquitination (Figure 3M). Conversely, loss of USP22 expression resulted in a significant increase in FoxM1 ubiquitination in both mouse 4T1 and patient-derived breast cancer cells (Figure 3N). These results define USP22 as a *de novo* FoxM1 deubiquitinase in breast cancer cells that protects FoxM1 from ubiquitination-mediated proteasomal degradation thereby upregulating integrin β1 expression.

USP22 promotes integrin β1 expression through FoxM1 stabilization

FoxM1 has been identified as an integrin β1 transcription factor thus promoting breast cancer progression.[26] Indeed, five consensually putative FoxM1 DNA-binding sites (C/TAAAC/TA)[30,31] were identified in ITGB1 promoter region (Figure 4A). Chromatin immunoprecipitation (ChIP) coupled with PCR amplification using specific primers demonstrated that FoxM1 binds to the region with putative binding site #1 and #3 (Figures 4A and 4B). In addition, the loss of USP22 resulted in a significant reduction in FoxM1 binding to ITGB1 promoter (Figures 4A and

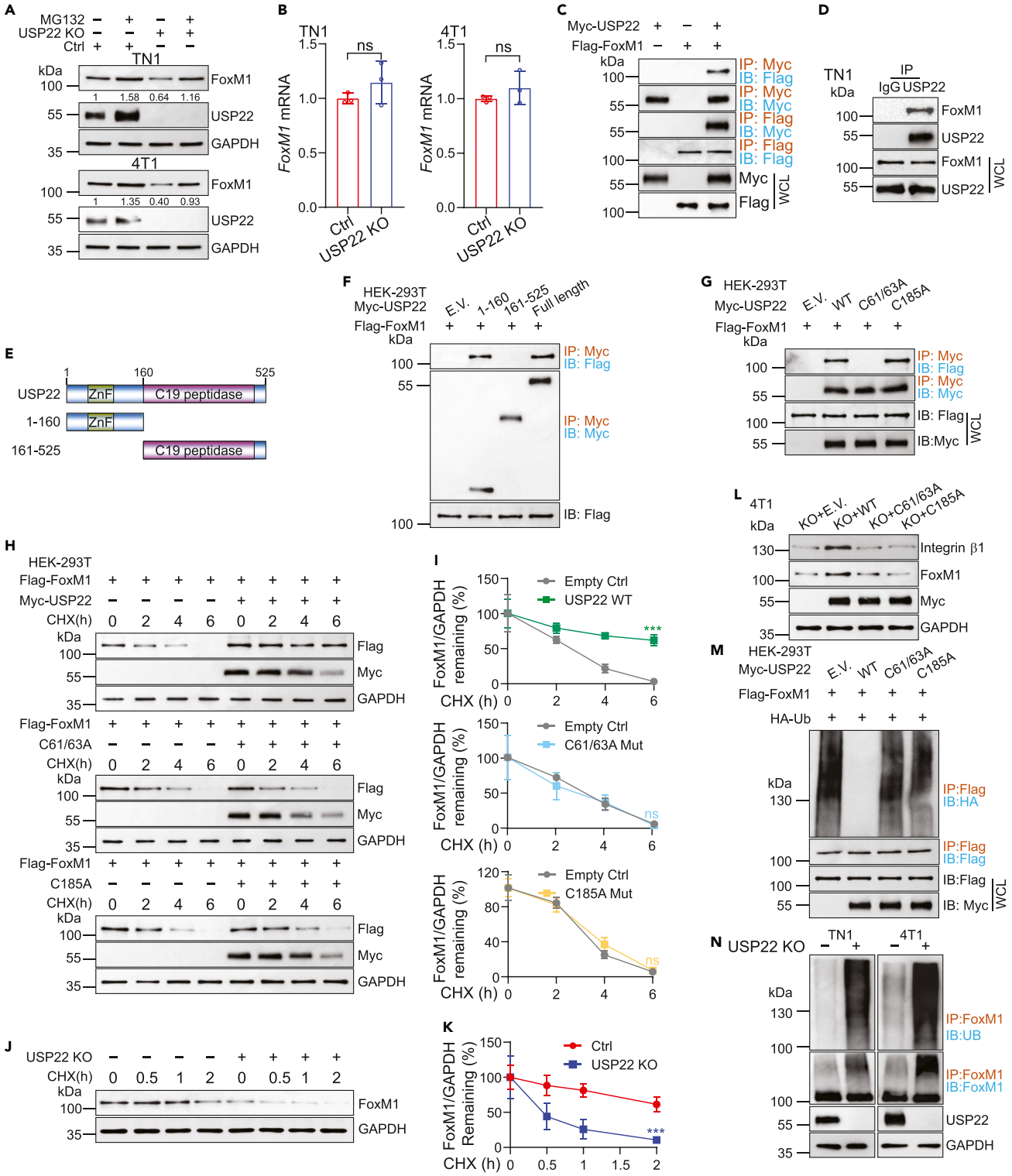

Figure 3. USP22 interacts with and stabilizes FoxM1

(A) TN1 and 4T1 stably expressing control or USP22 sgRNA were treated with or without the proteasome inhibitor MG132 (10 μM, 12 h) and then FoxM1 protein expression level was evaluated. Band intensities of FoxM1 were quantified and the results are expressed as FoxM1/GAPDH levels relative to control cells.

(B) Total RNA was isolated from TN1 and 4T1 cells stably expressing control or USP22 sgRNA. The mRNA levels of *FoxM1* were determined by real-time PCR. β-actin was used as an internal control. ns means no significant difference.

Figure 3. *Continued*

(C) Interaction of USP22 with FoxM1. HEK-293T cells were transiently transfected with FLAG-tagged FoxM1 and Myc-tagged USP22. Cell extracts were immunoprecipitated (IP) using primary antibodies against Myc and then subjected to immunoblotting (IB) analysis. WCL means whole-cell lysates.

(D) Endogenous USP22 and control IgG were immunoprecipitated from TN1 cell lysates and then subjected to immunoblotting for analyzing associated proteins. Rabbit IgG was used as the isotype control.

(E) Schematic representation of the N-terminal Myc-tagged full-length USP22, and various corresponding truncation mutants.

(F) HEK-293T cells were transfected with the indicated truncated constructs, followed by IP with Myc antibody and followed by immunoblot (IB) with antibodies against FLAG. EV means empty vector.

(G) HEK-293T cells were transiently transfected with FLAG-tagged FoxM1, HA-tagged ubiquitin and Myc-tagged USP22 or USP22 C61/63A, C185A mutant. Cell extracts were IP using primary antibodies against FLAG and then subjected to IB analysis to analyze FoxM1 ubiquitylation linkage.

(H) HEK-293T cells were co-transfected with FLAG-tagged FoxM1 and Myc-tagged USP22 WT or USP22 C61/63A, C185A mutant for 24 h, followed by treatment with 20 $\mu g\ mL^{-1}$ cycloheximide for the indicated times, and cell lysates were subjected to immunoblot with indicated antibodies. CHX means cycloheximide.

(I) Quantification showing that overexpression USP22 WT but not USP22 C61/63A, C185A mutant augments FoxM1 half-life. Quantification of FoxM1 relative to GAPDH was quantified by ImageJ. $n = 3$.

(J) 4T1 USP22-deficent or control cells were treated with 20 $\mu g\ mL^{-1}$ CHX for the indicated times and cell lysates were examined by immunoblotting.

(K) Quantification showing that USP22 ablation attenuates FoxM1 half-life. FoxM1 band intensity was quantified, and the results are expressed as FoxM1/GAPDH levels relative to untreated cells. $n = 3$.

(L) HEK-293T cells were transiently transfected with FLAG-tagged FoxM1 and Myc-tagged USP22 or USP22 C61/63A, C185A mutant. Cell extracts were IP using primary antibodies against Myc and then subjected to IB analysis.

(M) Immunoblot analyses of indicated proteins of 4T1 USP22-deficent cells transduced with USP22 WT or indicated mutants. Enforced expression of USP22 WT, but not indicated mutants, rescued the level of FoxM1 and integrin β1 in USP22-deficent cells.

(N) TN1 and 4T1 stably expressing control or USP22 sgRNA cell lysates were subjected to IP with FoxM1 antibody, followed by IB with antibodies against ubiquitin. Cells were treated with 10 μM MG132 for 12 h before harvesting. The error bars show the mean ± SD. The significances of differences between different group were determined by two-tailed Student's t test. *** indicates $p < 0.001$.

4B). Taken together with our results, this suggests a possibility that USP22 controls breast cancer cell *ITGB1* expression through FoxM1 stabilization. Indeed, reconstitution of FoxM1 expression fully restored the endogenous integrin β1 expression in both USP22-null 4T1 and $L2G^{+}$ TN1 breast cancer cells as determined by western blot (Figures 4C and 4D), which was further confirmed by flow cytometry (Figures 4E–4G).

In contrast, we observed that FoxM1 expression fails to rescue integrin β2-7 expression (Figure S4A). These results support our hypothesis that USP22 specifically promotes integrin β1 expression through FoxM1 stabilization. Consistent with this, we observed that ectopic expression of FoxM1 largely restored the tumor sphere formation ability of USP22-deficent breast cancer cells (Figures 4H–4J). Likewise, the impaired ability in colony formation of 4T1 breast cancer cells by USP22 depletion was largely rescued by exogenous FoxM1 expression (Figures S4B and S4C). Notably, we found that FoxM1 overexpression in 4T1 cells modestly enhanced tumor sphere formation ability and integrin β1 expression, suggesting that FoxM1 is potent regulator of integrin β1 (Figures S4D–S4F).

We also noticed that, while FoxM1 re-expression fully rescued integrin β1 expression both in USP22-null 4T1 and TN1 breast cancer cells, it only partially restores their sphere and colony formation (Figures 4H–4J). We then utilized the lung metastasis model to further illustrate the role of USP22-FoxM1-integrin β1 pathway in breast cancer tumorigenesis in BALB/c mice. Indeed, contrasting the effect of USP22 deletion which resulted in a greater than 50% reduction in lung metastases 4T1 cancer nodules, FoxM1 re-introduction restored USP22-null 4T1 cancer lung metastasis to a level of about 85–90% of the WT (Figures 4K–4M). Consequently, FoxM1 expression attenuated but not totally abolished the protection of mice from lung metastasis-induced lethality by USP22 targeted inhibition (Figure 4N). Collectively, these results support that USP22 promotes breast cancer metastasis partially through promoting FoxM1-mediated integrin β1 expression.

Pharmacological inhibition of USP22 abrogates BCSCs tumorigenicity

Our discovery that genetic USP22 deletion hindered breast BCSCs self-renewal and inhibited their lung metastasis provides a rationale for USP22 targeting in anticancer therapy. We first analyzed the effects of pharmacological USP22 inhibition on BCSCs self-renewal using a small molecule inhibitor USP22i-S02 (S02) that we recently identified.[32] Consistent with our observation from USP22 CRISPR knockout studies, treatment of breast cancer cells 4T1 and TN1 significantly inhibited both integrin β1 and FoxM1 expression. Consistent with our previous observations, S02 treatment also reduced USP22 expression levels owing to USP22 maybe a deubiquitinase of itself (Figure 5A; Figure S5A). Further addition of the proteasomal inhibitor MG132, but not with lysosome inhibitor NH_4Cl, largely rescued FoxM1 protein levels from S02 treatment (Figures S5B and S5C), confirming our observation that USP22 inhibition facilitates proteasomal FoxM1 protein degradation. In line with this, treatment of 4T1 cells with S02 shortened FoxM1 protein half-life (Figures S5D and S5E). As expected, S02 treatment suppressed *ITGB1* and other stemness related genes expression, including *CD44*, *ALDH*, and *NANOG* (Figure 5B). In contrast, S02 treatment did not alter *FoxM1* mRNA transcription (Figure S5F). These results confirm that USP22 is a positive regulator for FoxM1-mediated *ITGB1* expression in breast cancer cells by an orthogonal pharmacological approach.

We next sought to determine the effects of USP22 pharmacological inhibition on BCSCs self-renewal, with the obvious fact that S02 treatment presented reduced BCSCs population by more than 80%, a level that is comparable to USP22 knockout (Figures 5C and S5G). Importantly, S02 treatment of USP22-null breast cancer cells did not further reduce the frequency of BCSCs (Figures 5C and S5G), supporting the high specificity of this USP22-specific small molecule inhibitor. Consequently, treatment with S02 significantly impaired breast cancer cell sphere and colony formation capability (Figures 5D, 5E, S5H, and S5I). Further *in vitro* extreme limiting dilution assay confirmed that S02

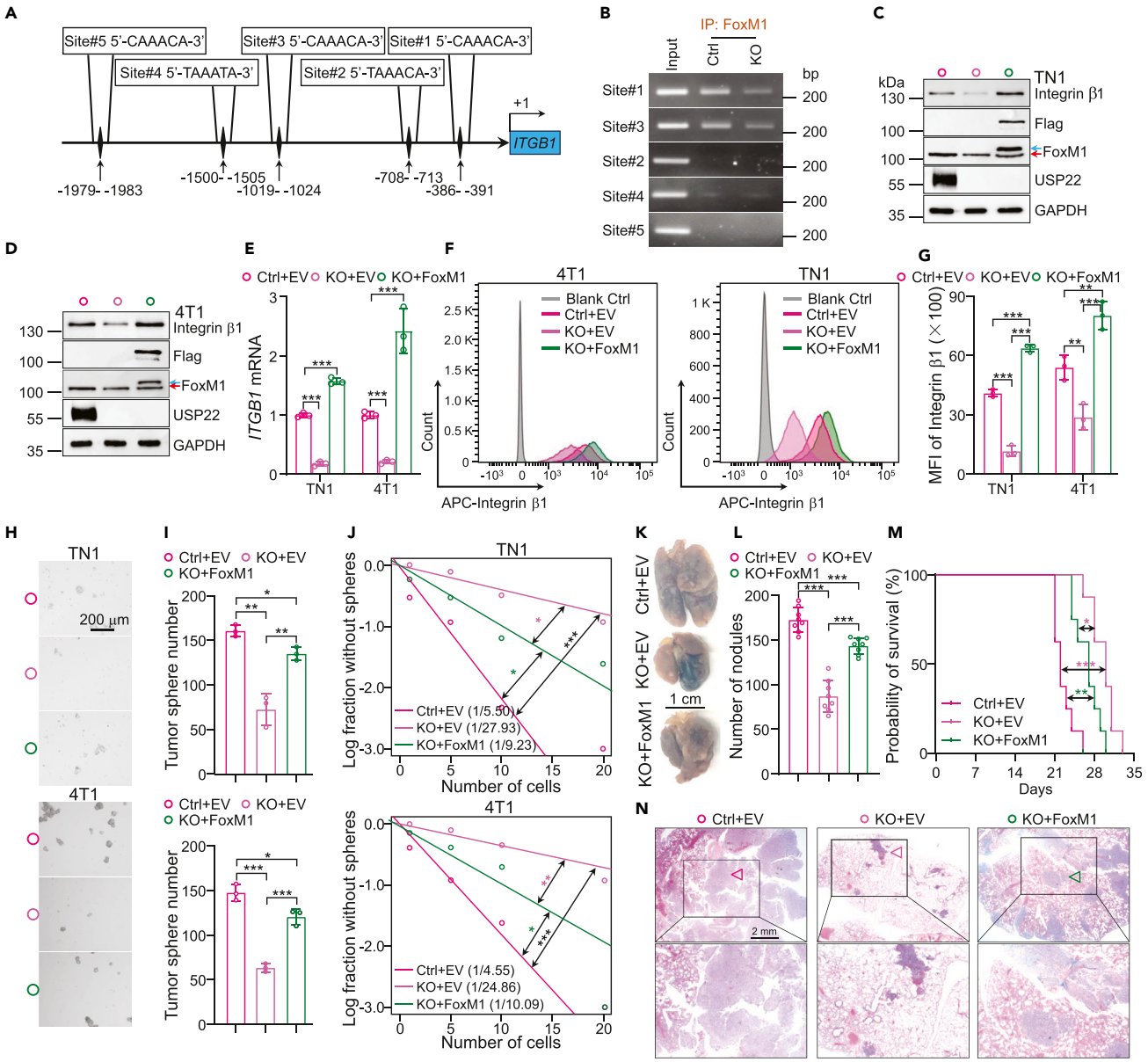

Figure 4. FoxM1 introduction partially rescues the suppressive effects caused by USP22 depletion

(A) Schematic illustration of putative FoxM1 binding sites in *ITGB1* promoter. +1 indicates transcription start site.

(B) USP22 depletion or control cells were subjected to chromatin immunoprecipitation (ChIP) assay, and the ChIP products were amplified by quantitative reverse-transcription PCR (RT-qPCR). Input was used as positive control. bp indicates base pairs.

(C and D) Immunoblot analysis of integrin β1, Flag and USP22 in TN1 and 4T1 cells transduced with Flag-FoxM1 in the setting of depleted USP22. Enforced expression of FoxM1 completely rescued the protein level of integrin β1 in USP22-deficent cells. Red and Blue arrow indicate endogenous and exogenous FoxM1 proteins, respectively.

(E) The mRNA levels of *ITGB1* in TN1 and 4T1 cells were determined by real-time PCR. Enforced expression of FoxM1 rescued the mRNA level of *ITGB1* in USP22-deficent cells. β-actin was used as an internal control.

(F) Ectopic expression of FoxM1 completely rescued the protein level of integrin β1 in USP22-deficent cells determined by flow cytometry. Representative FACS data are shown.

(G) Quantification showing that ectopic expression of FoxM1 completely rescued the protein level of integrin β1 in USP22-deficent cells.

(H) Tumor sphere formed from TN1 and 4T1 cells transduced with FLAG-FoxM1 in the setting of depleted USP22. The representative images of tumor sphere are shown. Scale bar, 500 μm.

(I) Quantifications showing that FoxM1 expression partially rescues the decreased tumor sphere formation ability caused by USP22 depletion.

Figure 4. *Continued*

(J) The frequencies of tumor sphere formation of TN1 and 4T1 cells expressing FLAG-FoxM1 or empty control in the setting of USP22 deficiency determined by *in vitro* extreme dilution analysis. The significance of the difference between the indicated groups was evaluated by χ^2 test. $n = 10$. The frequency of CSCs was shown.

(K) Representative images of lungs from mice injected 4T1 cells expressing either control or USP22 sgRNA in combination with vector control or FLAG-FoxM1. Scale bar 1 cm.

(L) Quantification result showing that introduction of FLAG-FoxM1 partially rescues the inhibitory effects caused by USP22 depletion.

(M) H&E staining of lung metastasis from indicated group. Scale bar, 2 mm.

(N) Kaplan-Meier survival curves of mice implanted with indicated cells. Quantification showing that ectopic expression of FoxM1 in 4T1 USP22-deficient cells shorten mice survival compared to USP22-deficient cells. Significance testing was done by log-rank test. The error bars show the mean ± SD. The significances of differences between groups were determined by two-tailed Student's t test. *, **, *** indicates $p < 0.05$, $p < 0.01$, $p < 0.001$, respectively.

inhibited BCSCs self-renewal (Figure 5F). Moreover, we sorted BCSCs ($CD24^{-}CD44^{+}$, defined as TN1 BCSCs) and non-CSCs ($CD24^{+}CD44^{-}$, defined as TN1 non-BCSCs) from TN1 cells as shown in Figure 1A and treated with escalating S02. Intriguingly, S02 treatment preferentially eliminated BCSCs, reflected by the increased IC_{50} of BCSCs compared to non-BCSCs (Figure 5G), suggesting a promising therapeutic potential in the treatment of breast cancer. We then used the preclinical 4T1 breast pulmonary metastasis model to illustrate the potential anti-metastatic effect of S02 (Figure S5J). Of note, a six-day treatment with S02 after tail vein injection of 4T1 breast cancer cells resulted in a significant reduction in 4T1 breast cancer lung metastasis and prolonged mice survival (Figures 5H–5K). Further IHC staining of the lung metastatic cancers detected a reduction in both integrin β1 and USP22 levels in the S02 treatment groups (Figures 5L and S5K). Consistent with our previous report, administration of S02 did not show any detectable toxicity as the mice body weight was unaltered (Figure S5L), and further hematoxylin-eosin (H&E) staining did not detect obvious liver damage in S02 treatment mice (Figure S5M). Therefore, these results indicate that pharmacological USP22 targeting is a safe and effective therapy in treatment of triple negative breast cancers.

We then further evaluated the therapeutic potential of USP22i-S02 using a patient-derived xenograft (PDX) model by orthotopically implanting TN1 cells in immune compromised RAG1 deficient mice (Figure 5M). Intriguingly, a 3-day treatment with pre-established PDX tumor significantly hindered PDX tumor growth (Figures 5N and 5O). Further characterization by IHC staining showed a reduction in levels of USP22, FoxM1 and integrin β1 protein expression when treated with USP22i-S02, which consequently inhibited breast cancer cell growth indicated by the decrease in the percentage of Ki-67^{+} proliferative cells (Figure S5N). Importantly, we detected a significant reduction in $CD44^{+}$ breast cancer cells in the S02 treated group, implying that USP22 pharmacological inhibition attenuates either the BCSCs self-renewal or their survival (Figure 5P). Therefore, pharmacological inhibition of USP22 suggests a potentially efficacious treatment for breast cancer and metastasis.

Positive correlation of USP22, FoxM1, and integrin β1 in human breast cancer

Our data collectively demonstrates that USP22 maintains breast cancer stemness in part through stabilizing *ITGB1* transcription factor FoxM1 to promote breast cancer growth and metastasis, therefore defining a previously unknown USP22-FoxM1-*ITGB1* pathway in breast cancer pathogenesis. Further analysis of the sorted integrin $\beta1^{low}$, integrin $\beta1^{middle}$, and integrin $\beta1^{high}$ 4T1 cells revealed a gradual elevation in USP22 and FoxM1 expressions (Figures 6A and 6B). We then generated 4T1 cells expressing a green fluorescent protein (GFP)-USP22 fusion protein without the endogenous USP22 (Figure 6C). Consistently, the expression of both FoxM1 and *ITGB1* are profoundly increased in $USP22^{high}$ compared to that of $USP22^{low}$ 4T1 knock-in cells (Figures 6D and 6E). Furthermore, a significant increase in integrin β1 and FoxM1 in the BCSCs versus the non-BCSCs population was observed (Figure 6F).

To further investigate the critical roles of the USP22-FoxM1-integrin β1 axis in breast cancer pathogenesis, we utilized IHC staining to determine the expression of USP22, FoxM1, and integrin β1 protein in human breast cancer tissue microarray (Table S1). As expected, the protein levels of USP22, FoxM1, and integrin β1 was markedly higher in the breast tumor tissues than those in benign tumors (Figures 6G, 6H, and S6A–S6D; Table S1) and even further elevated in metastatic tissues (Figures 6G and 6H; Table S2). This further corroborates our discovery that up-regulation of USP22 in BCSCs promotes breast cancer lung metastasis through FoxM1-mediated *ITGB1* gene transcription. To support this notion, we found that the protein expression levels of USP22, FoxM1 and integrin β1 are strongly correlated in human breast cancers (Figures 6I and S6E). Collectively, our study identifies USP22 as a FoxM1-specific deubiquitinase thereby enhancing FoxM1 mediated transcriptional activation of *ITGB1* expression which promotes BCSCs self-renewal and drives breast cancer metastasis to distal organs (Figure 6J).

DISCUSSION

Our study defines a previously unknown USP22-FoxM1-integrin β1 pathway critically important for both mouse and human BCSCs self-renewal. We arrive at this conclusion through the following discoveries: first, USP22 is further upregulated in BCSCs and breast cancer and targeted USP22 deletion impaired BCSCs self-renewal and tumorigenicity. Secondly, USP22 controls breast cancer cell stemness through integrin β1 upregulation. Third, USP22 functions as a bona fide deubiquitinase of the *ITGB1* transcription FoxM1 and promotes BCSCs self-renewal through FoxM1-mediated integrin β1 expression. Fourth, pharmacological USP22 inhibition impairs BCSCs self-renewal and protects mice from breast cancer lung metastasis-induced mortality. Last but not least, USP22 and *ITGB1* are positively correlated in more than 90% of human cancer types, and USP22, integrin β1, and FoxM1 levels are increased and positively correlated in breast cancers.

Integrins play critical roles in supporting the function of both normal adult stem cells and their neoplastic derivatives.[33] While integrin mutations are rarely identified, most of, if not all integrin family members are often upregulated in CSCs and this upregulation often promotes

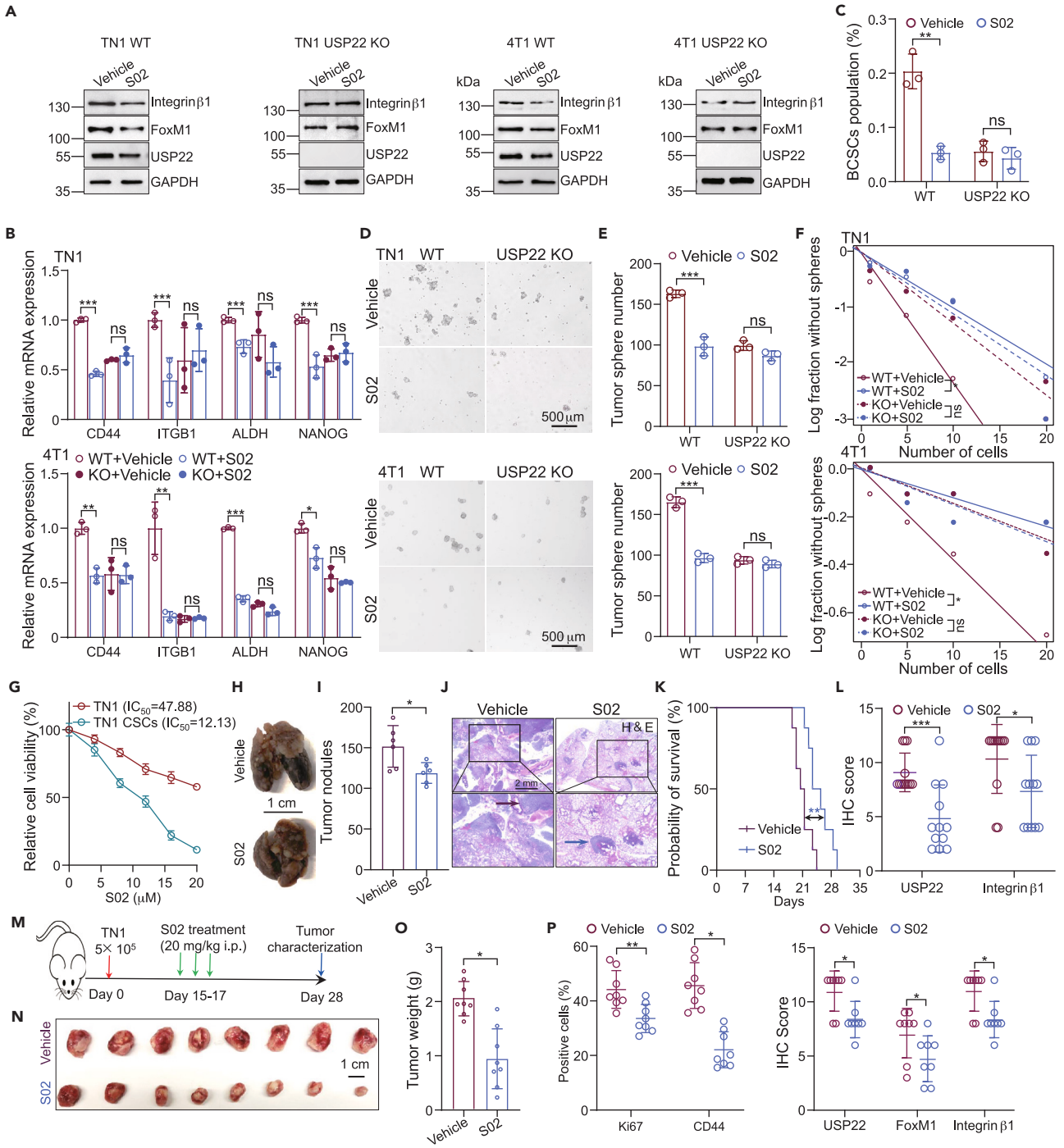

Figure 5. The USP22 inhibitor attenuates BCSCs self-renewal

(A) TN1 and 4T1 WT or USP22-null cells were treated with or without 20 μM S02 for 24 h. Cell lysates were analyzed by immunoblotting using the indicated antibodies. Dimethyl sulfoxide (DMSO) was used as a vehicle control.

(B) TN1 and 4T1 WT or USP22 depletion cells were treated with or without 20 μM S02 for 48 h. The mRNA levels of indicated genes in TN1 and 4T1 cells were determined by real-time PCR. β-actin was used as an internal control.

(C) 4T1 WT or USP22-null cells were treated with or without 20 μM S02 for 48 h, the cells were subsequently stained with CD44 and CD24 antibodies, and then analyzed by flow cytometry. S02 treatment decreases BCSCs ($CD44^+CD24^-$) population determined by flow cytometry. Quantification data are shown.

(D) Tumor sphere formation ability was evaluated in TN1 and 4T1 cells treated with or without 20 μM S02 for 10 days. Representative images of each group are shown. Scale bars, 500 μm.

Figure 5. *Continued*

(E) Quantification showing that tumor sphere formation ability was restricted by S02 treatment in TN1 and 4T1 WT but not USP22-deficient cells.

(F) *In vitro* extreme limiting dilution assay by plating gradient numbers of TN1 and 4T1 control or USP22 ablation cells showed the frequencies of tumor sphere formation in indicated cells treated with or without 20 μM S02 for 10 days. The frequency of CSCs was shown.

(G) S02 treatment preferentially inhibits BCSCs cell viability compared to non-BCSCs.

(H) Representative images of lungs from mice given intravenous injection of 5×10^4 4T1 cells. 24 h later, mice were randomized into treatment groups and treated with S02 (10 mg/kg), or vehicle control by intraperitoneal injection six times (once every day).

(I) Tumor nodules on the lungs of mice injected with S02 or vehicle control. Scale bar, 1 cm.

(J) The mice were humanely sacrificed after 20 days injection of 4T1 cells. The H&E staining sections show representative metastatic tumor. Scale bar, 2 mm.

(K) 4T1 cells (5×10^4 cells per mouse) were intravenously injected into BALB/c mice. Mice were treated as described in J. The survival of mice was evaluated ($n = 8$. Kaplan-Meier plotter with two-sided log rank test).

(L) Immunohistochemical staining of sections from nodules in the lung as in H stained with antibody against USP22 and integrin β1.

(M) The scheme for mouse breast cancer treatment model. TN1 cells (5×10^4 cells per mouse) were orthotopically injected into NOD/SCG mice. Two weeks later when the tumors were around 100 mm^3, mice were randomized into treatment groups and treated with S02 (20 mg/kg) or vehicle control by intraperitoneal injection six times (twice a day).

(N) Images of xenograft tumors after orthotopically injecting TN1 cells and treated with vehicle or S02 by the indicated conditions. Scale bar, 1 cm

(O) Weights of xenograft tumor treated with vehicle or S02.

(P) Immunohistochemical analysis of sections from xenograft tumors treated with vehicle or S02 stained with indicated antibodies. Three individual samples were analyzed, and quantification data are shown. The error bars show the mean ± SD. The significances of differences between groups were determined by two-tailed Student's t test. *, **, *** indicates $p < 0.05$, $p < 0.01$, $p < 0.001$, respectively.

CSCs self-renewal, cancer initiation and metastasis.[19,34,35] Several tumor initiating and/or promoting pathways including epidermal growth factor (EGF) and vascular endothelial growth factor-mediated signaling pathways activate the RAS-MAP kinase cascade for *ITGB1* transcription through downstream AP-1 family transcription factors. On the other hand, the tumoral immune suppressive cytokine, transforming growth factor β, promotes β1 integrin expression through canonical SMAD family transcription factor activation. In addition, the forkhead box family transcription factors, both FoxO3 and FoxM1 have been identified to promote cancer invasion by promoting integrin β1.[26,36] Herein we define the USP22-FoxM1-integrin β1 axis as a critical regulatory node in the control of BCSCs self-renewal, tumor initiation and metastasis. In addition to integrin β1, USP22 appears to promote the transcription of several additional integrin family members. However, FoxM1 reconstitution only rescued integrin β1 expression, implying that USP22 regulates integrin family members via distinct molecular mechanisms. FoxM1 has been also known to be a crucial transcription factor for the maintenance of a variety of human CSCs and its expression is associated with a worse clinical prognosis.[37–39] Therefore, this study links three important CSCs genes teaming together to maintain an optimal BCSCs pool. Importantly, our unbiased analysis of CCLE database revealed a significant positive correlation between USP22 and *ITGB1* in breast cancer cell lines, suggesting that the USP22-FoxM1-integrin β1 axis is a common mechanism of CSCs self-renewal.

We also noted that while integrin β1 expression is fully restored in USP22-null mouse and human breast cancer cells, FoxM1 expression only achieved a partial rescue in their *in vitro* tumor sphere formation and *in vivo* lung metastasis, indicating that USP22 exerts its function in part through an integrin β1-independent manner. Indeed, it has been shown that USP22 promotes hypoxia-induced hepatocellular carcinoma stemness through a HIF-1α/USP22 positive feedback loop upon TP53 inactivation.[40] On the other hand, USP22 regulates embryonic stem cell differentiation via transcriptional repression of sex-determining region Y-box 2 (SOX2).[41] Therefore, USP22 appears to play a diverse role in regulating cell stemness in both physiological and pathological contexts.

Our study provides a strong rationale for targeting the USP22-FoxM1-integrin β1 pathway in anticancer therapy as pharmacological USP22 inhibition reduced the frequency of BCSCs and attenuated both mouse and human invasive breast cancer lung metastasis. In addition to its cancer cell-intrinsic roles, USP22 has been recently discovered to suppress tumor immunosurveillance through potentiating $Foxp3^+$ regulatory functions[32,42] as well as upregulating the expression of checkpoint receptors PD-L1 and CD73.[43,44] Therefore, targeting USP22 presumably achieves both chemo- and immuno-therapeutic efficacy. Additionally, therapeutics that are either specific antibody or peptide inhibitors of integrin family members have been tested for antitumor therapy and are currently in several ongoing clinical trials. The anti-α5β1 integrin antibody volociximab was shown to inhibit angiogenesis and suppress tumor growth and metastasis in mice and shows some antitumor efficacy in the treatment of advanced non-small-cell lung cancer and in pancreatic cancer.[45,46] To date, clinical trials that integrin-based drugs designed to platelet integrins to prevent blood clotting or anti integrin αv-based reagents designed to block angiogenesis in cancer have met with limited success.[47–49] It has been documented that integrin β1 plays essential roles in every steps of cancer development.[50] Therefore, the development of integrin β1 based treatment in cancers is urgent needed.

Limitations of the study

Directly targeting integrin β1 is likely achieving very limited success as integrin β1 is highly expressed in a variety of non-cancer cells and is required for critical biological functions including normal mammary stem cells maintenance. Although we discovered that USP22-FoxM1-integrin β1 pathway is critical for breast cancer self-renewal and simultaneously targeting USP22 and specific integrin β1 heterodimer(s) targeting may achieve a synergistic efficacy in combating human cancers, leading to reduced therapeutic doses and side effects. As integrin β1 forms heterodimer with individual integrin α subunit,[51–53] we have not identified which integrin α subunits are involved in heterodimerizing with integrin β1 to mediate the tumor suppressive effects elicited by USP22 ablation.[54] Given integrins can interact with a plethora of extracellular matrix proteins, such as fibrinogen, vitronectin, osteopontin, and fibronectin). We have not shown here the potential ligand of integrin

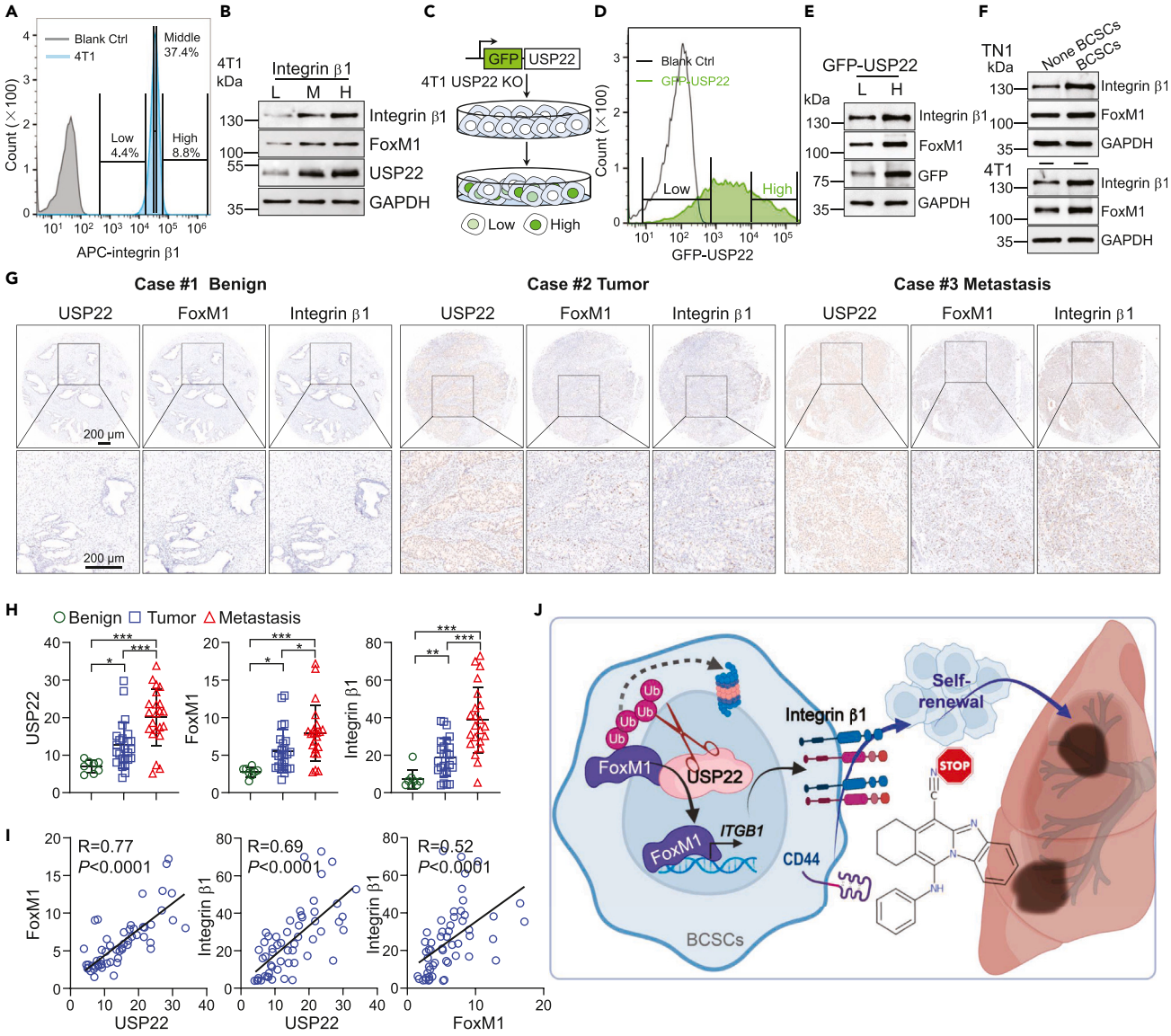

Figure 6. Clinical significance of USP22/FoxM1/Integrin β1 signaling axis in breast cancer

(A) Flow cytometry was used to isolate 4T1 cells with low, middle and high level of integrin β1.

(B) Immunoblot analysis for USP22, FoxM1, and integrin β1 in 4T1 cells isolated according to integrin β1 expression level. L, M, and H indicate 4T1 cells with low, middle, and high integrin β1 expression level, respectively.

(C) The scheme for GFP-USP22 knock-in 4T1 USP22 knockout cells.

(D) Flow cytometry sorting of GFP^{low} or GFP^{high} cells isolated from GFP-USP22 knock-in 4T1 USP22 knockout cells. Representative flow cytometric data are shown.

(E) Immunoblot analysis for FoxM1 and integrin β1 of USP22 knock-in 4T1 USP22 knockout cells isolated according to GFP intensity.

(F) BCSCs and non-BCSCs were isolated from TN1 and 4T1 cells, respectively. The cell extracts were analyzed by immunoblotting using FoxM1 and integrin β1 antibody.

(G) Immunohistochemical staining of tissue microarray #1 including 55 specimens (n = 8 breast benign specimens, n = 20 breast cancer specimens, and n = 22 metastatic specimens) for USP22, FoxM1 or integrin β1. Representative consecutive sections from 3 specimens are shown. Scale bars: 200 μm. The clinicopathological characteristics of tissue microarrays are shown in Table S1.

(H) The integrated optical density of USP22 (left panel), FoxM1 (middle panel), or integrin β1 (right panel) was compared with those in indicated groups.

(I) Linear regression analysis of the integrated optical density of USP22 and FoxM1 (left panel), USP22 and integrin β1 (middle panel), and FoxM1 and integrin β1 (right panel) showed a significant positive correlation. Pearson's R correlation test and the Pearson correlation coefficients are shown in the matrix. n = 55.

(J) Proposed working model. USP22 functions as a *de novo* FoxM1 deubiquitinase, which plays essential roles in triggering transcriptional activation of *ITGB1*, thereby promoting BCSCs self-renewal and driving breast cancer metastasis. The error bars show the mean ± SD. The significances of differences between groups were determined by two-tailed Student's t test. *, **, *** indicates $p < 0.05$, $p < 0.01$, $p < 0.001$, respectively.

β1. Thus, it will be important to identify the specific integrin alpha chain(s) heterodimerizing with integrin β1 chain to mediate these effects elicited by USP22 as well as the ligands involved.

STAR★METHODS

Detailed methods are provided in the online version of this paper and include the following:

- KEY RESOURCES TABLE
- RESOURCE AVAILABILITY
  - Lead contact
  - Materials availability
  - Data and code availability
- EXPERIMENTAL MODEL AND STUDY PARTICIPANT DETAILS
  - Human breast cancer tissue microarray
- METHOD DETAILS
  - Cell culture
  - Molecular cloning and plasmid
  - Tumor sphere formation assay
  - Colony formation assay
  - Cell viability
  - *In vitro* extreme limiting dilution assay
  - Real-time PCR
  - Flow cytometry analysis and cell sorting
  - Immunoblot
  - Co-immunoprecipitation
  - Chromatin immunoprecipitation (Ch-IP) qPCR
  - Dual-luciferase assay
  - Immunohistochemistry
  - Tissue microarray
  - Animal studies
- QUANTIFICATION AND STATISTICAL ANALYSIS

SUPPLEMENTAL INFORMATION

Supplemental information can be found online at https://doi.org/10.1016/j.isci.2024.110592.

ACKNOWLEDGMENTS

We thank the Northwestern Lurie Cancer Center flow cytometry core for their service support. We thank Dr. Liping Jiang from the University of Illinois at Chicago for conducting the Dual-luciferase reporter assay. This work was supported by National Institutes of Health grants R01DK126908, R01DK120330, R01CA257520, and CA232347 (to D.F.), R01CA245699 and UG3CA256967 (to H.L.), National Natural Science Foundation of China (no.82073768) and Dalian High-level Talent Innovation Support Program (no. 2019RD03) to Z.S., Department of Defense Breast Cancer Research Program W81XWH2010679 (to H.L), and Lynn Sage Breast Cancer Foundation (D.F. and H.L.).

AUTHOR CONTRIBUTIONS

D.F. designed and supervised this study and wrote the manuscript. K.L. performed most of the experiments and wrote the manuscript. Q.G. developed the concepts and assisted with K.L. in this study. H.L. and Y. J. provided breast cancer patient-derived xenograft models. J.W. and Y. J. helped with the animal studies. A.T. and N.L.M. helped with the flow cytometry experiments, R.I, B.G., W.L., and Z.S. helped with the data analysis. H.L., S.M.C., A.T. B.Z., and R.I. edited the manuscript.

DECLARATION OF INTERESTS

Drs. Deyu Fang and Huiping Liu are co-founders and equity owners of ExoMira Medicine Inc. Dr. Fang is the inventor of USP22 inhibitor-S02 (patent #: 63/201330).

Received: January 9, 2024
Revised: April 28, 2024
Accepted: July 24, 2024
Published: July 27, 2024

REFERENCES

1. Ganesh, K., and Massagué, J. (2021). Targeting metastatic cancer. Nat. Med. *27*, 34–44. https://doi.org/10.1038/s41591-020-01195-4.
2. Valastyan, S., and Weinberg, R.A. (2011). Tumor metastasis: molecular insights and evolving paradigms. Cell *147*, 275–292. https://doi.org/10.1016/j.cell.2011.09.024.
3. Lytle, N.K., Barber, A.G., and Reya, T. (2018). Stem cell fate in cancer growth, progression and therapy resistance. Nat. Rev. Cancer *18*, 669–680. https://doi.org/10.1038/s41568-018-0056-x.
4. Prager, B.C., Xie, Q., Bao, S., and Rich, J.N. (2019). Cancer Stem Cells: The Architects of the Tumor Ecosystem. Cell Stem Cell *24*, 41–53. https://doi.org/10.1016/j.stem.2018.12.009.
5. Weber, G.F., Ashkar, S., and Cantor, H. (1997). Interaction between CD44 and osteopontin as a potential basis for metastasis formation. Proc. Assoc. Am. Physicians *109*, 1–9.
6. Liu, X., Taftaf, R., Kawaguchi, M., Chang, Y.F., Chen, W., Entenberg, D., Zhang, Y., Gerratana, L., Huang, S., Patel, D.B., et al. (2019). Homophilic CD44 Interactions Mediate Tumor Cell Aggregation and Polyclonal Metastasis in Patient-Derived Breast Cancer Models. Cancer Discov. *9*, 96–113. https://doi.org/10.1158/2159-8290.CD-18-0065.
7. Glinsky, G.V., Berezovska, O., and Glinskii, A.B. (2005). Microarray analysis identifies a death-from-cancer signature predicting therapy failure in patients with multiple types of cancer. J. Clin. Invest. *115*, 1503–1521. https://doi.org/10.1172/JCI23412.
8. Zhang, Y., Yao, L., Zhang, X., Ji, H., Wang, L., Sun, S., and Pang, D. (2011). Elevated expression of USP22 in correlation with poor prognosis in patients with invasive breast cancer. J. Cancer Res. Clin. Oncol. *137*, 1245–1253. https://doi.org/10.1007/s00432-011-0998-9.
9. Prokakis, E., Dyas, A., Grün, R., Fritzsche, S., Bedi, U., Kazerouni, Z.B., Kosinsky, R.L., Johnsen, S.A., and Wegwitz, F. (2021). USP22 promotes HER2-driven mammary carcinoma aggressiveness by suppressing the unfolded protein response. Oncogene *40*, 4004–4018. https://doi.org/10.1038/s41388-021-01814-5.
10. Lin, Z., Yang, H., Kong, Q., Li, J., Lee, S.M., Gao, B., Dong, H., Wei, J., Song, J., Zhang, D.D., and Fang, D. (2012). USP22 Antagonizes p53 Transcriptional Activation by Deubiquitinating Sirt1 to Suppress Cell Apoptosis and Is Required for Mouse Embryonic Development. Mol. Cell *46*, 484–494. https://doi.org/10.1016/j.molcel.2012.03.024.
11. Lin, Z., Tan, C., Qiu, Q., Kong, S., Yang, H., Zhao, F., Liu, Z., Li, J., Kong, Q., Gao, B., et al. (2015). Ubiquitin-specific protease 22 is a deubiquitinase of CCNB1. Cell Discov. *1*, 15028. https://doi.org/10.1038/celldisc.2015.28.
12. Zhang, X.Y., Varthi, M., Sykes, S.M., Phillips, C., Warzecha, C., Zhu, W., Wyce, A., Thorne, A.W., Berger, S.L., and McMahon, S.B. (2008). The putative cancer stem cell marker USP22 is a subunit of the human SAGA complex required for activated transcription and cell-cycle progression. Mol. Cell *29*, 102–111. https://doi.org/10.1016/j.molcel.2007.12.015.
13. Liu, H., Liu, N., Zhao, Y., Zhu, X., Wang, C., Liu, Q., Gao, C., Zhao, X., and Li, J. (2019). Oncogenic USP22 supports gastric cancer growth and metastasis by activating c-Myc/NAMPT/SIRT1-dependent FOXO1 and YAP signaling. Aging (Albany NY) *11*, 9643–9660. https://doi.org/10.18632/aging.102410.
14. Atanassov, B.S., Evrard, Y.A., Multani, A.S., Zhang, Z., Tora, L., Devys, D., Chang, S., and Dent, S.Y.R. (2009). Gcn5 and SAGA regulate shelterin protein turnover and telomere maintenance. Mol. Cell *35*, 352–364. https://doi.org/10.1016/j.molcel.2009.06.015.
15. Gennaro, V.J., Stanek, T.J., Peck, A.R., Sun, Y., Wang, F., Qie, S., Knudsen, K.E., Rui, H., Butt, T., Diehl, J.A., and McMahon, S.B. (2018). Control of CCND1 ubiquitylation by the catalytic SAGA subunit USP22 is essential for cell cycle progression through G1 in cancer cells. Proc. Natl. Acad. Sci. USA *115*, E9298–E9307. https://doi.org/10.1073/pnas.1807704115.
16. Kosinsky, R.L., Helms, M., Zerche, M., Wohn, L., Dyas, A., Prokakis, E., Kazerouni, Z.B., Bedi, U., Wegwitz, F., and Johnsen, S.A. (2019). USP22-dependent HSP90AB1 expression promotes resistance to HSP90 inhibition in mammary and colorectal cancer. Cell Death Dis. *10*, 911. https://doi.org/10.1038/s41419-019-2141-9.
17. Melo-Cardenas, J., Zhang, Y., Zhang, D.D., and Fang, D. (2016). Ubiquitin-specific peptidase 22 functions and its involvement in disease. Oncotarget *7*, 44848–44856. https://doi.org/10.18632/oncotarget.8602.
18. Hamidi, H., and Ivaska, J. (2018). Every step of the way: integrins in cancer progression and metastasis. Nat. Rev. Cancer *18*, 533–548. https://doi.org/10.1038/s41568-018-0038-z.
19. Gao, Q., Sun, Z., and Fang, D. (2023). Integrins in human hepatocellular carcinoma tumorigenesis and therapy. Chin. Med. J. *136*, 253–268. https://doi.org/10.1097/CM9.0000000000002459.
20. Pérez-Núñez, I., Rozalen, C., Palomeque, J.A., Sangrador, I., Dalmau, M., Comerma, L., Hernandez-Prat, A., Casadevall, D., Menendez, S., Liu, D.D., et al. (2022). LCOR mediates interferon-independent tumor immunogenicity and responsiveness to immune-checkpoint blockade in triple-negative breast cancer. Nat. Cancer *3*, 355–370. https://doi.org/10.1038/s43018-022-00339-4.
21. Liu, K., Jiang, L., Shi, Y., Liu, B., He, Y., Shen, Q., Jiang, X., Nie, Z., Pu, J., Yang, C., and Chen, Y. (2022). Hypoxia-induced GLT8D1 promotes glioma stem cell maintenance by inhibiting CD133 degradation through N-linked glycosylation. Cell Death Differ. *29*, 1834–1849. https://doi.org/10.1038/s41418-022-00969-2.
22. Ramos, E.K., Hoffmann, A.D., Gerson, S.L., and Liu, H. (2017). New Opportunities and Challenges to Defeat Cancer Stem Cells. Trends Cancer *3*, 780–796. https://doi.org/10.1016/j.trecan.2017.08.007.
23. Oskarsson, T., Batlle, E., and Massagué, J. (2014). Metastatic stem cells: sources, niches, and vital pathways. Cell Stem Cell *14*, 306–321. https://doi.org/10.1016/j.stem.2014.02.002.
24. Pang, R., Law, W.L., Chu, A.C.Y., Poon, J.T., Lam, C.S.C., Chow, A.K.M., Ng, L., Cheung, L.W.H., Lan, X.R., Lan, H.Y., et al. (2010). A subpopulation of CD26+ cancer stem cells with metastatic capacity in human colorectal cancer. Cell Stem Cell *6*, 603–615. https://doi.org/10.1016/j.stem.2010.04.001.
25. Klonisch, T., Wiechec, E., Hombach-Klonisch, S., Ande, S.R., Wesselborg, S., Schulze-Osthoff, K., and Los, M. (2008). Cancer stem cell markers in common cancers - therapeutic implications. Trends Mol. Med. *14*, 450–460. https://doi.org/10.1016/j.molmed.2008.08.003.
26. Hamurcu, Z., Kahraman, N., Ashour, A., and Ozpolat, B. (2017). FOXM1 transcriptionally regulates expression of integrin beta 1 in triple-negative breast cancer. Breast Cancer Res. Treat. *163*, 485–493. https://doi.org/10.1007/s10549-017-4207-7.
27. Zhou, A., Lin, K., Zhang, S., Chen, Y., Zhang, N., Xue, J., Wang, Z., Aldape, K.D., Xie, K., Woodgett, J.R., and Huang, S. (2016). Nuclear GSK3 beta promotes tumorigenesis by phosphorylating KDM1A and inducing its deubiquitylation by USP22. Nat. Cell Biol. *18*, 954–966. https://doi.org/10.1038/ncb3396.
28. Lin, Z., Yang, H., Tan, C., Li, J., Liu, Z., Quan, Q., Kong, S., Ye, J., Gao, B., and Fang, D. (2013). USP10 Antagonizes c-Myc Transcriptional Activation through SIRT6 Stabilization to Suppress Tumor Formation. Cell Rep. *5*, 1639–1649. https://doi.org/10.1016/j.celrep.2013.11.029.
29. Chen, Y., Li, Y., Xue, J., Gong, A., Yu, G., Zhou, A., Lin, K., Zhang, S., Zhang, N., Gottardi, C.J., and Huang, S. (2016). Wnt-induced deubiquitination FoxM1 ensures nucleus beta-catenin transactivation. Embo J. *35*, 668–684. https://doi.org/10.15252/embj.201592810.
30. Korver, W., Roose, J., and Clevers, H. (1997). The winged-helix transcription factor Trident is expressed in cycling cells. NUCLEIC Acids Res. *25*, 1715–1719. https://doi.org/10.1093/nar/25.9.1715.
31. Pierrou, S., Hellqvist, M., Samuelsson, L., Enerbäck, S., and Carlsson, P. (1994). Cloning and characterization of seven human forkhead proteins: binding site specificity and DNA bending. EMBO J. *13*, 5002–5012. https://doi.org/10.1002/j.1460-2075.1994.tb06827.x.
32. Montauti, E., Weinberg, S.E., Chu, P., Chaudhuri, S., Mani, N.L., Iyer, R., Zhou, Y., Zhang, Y., Liu, C., Xin, C., et al. (2022). A deubiquitination module essential for T_{reg} fitness in the tumor microenvironment. Sci. Adv. *8*, eabo4116. https://doi.org/10.1126/sciadv.abo4116.
33. Plaks, V., Kong, N., and Werb, Z. (2015). The Cancer Stem Cell Niche: How Essential Is the Niche in Regulating Stemness of Tumor Cells? Cell Stem Cell *16*, 225–238. https://doi.org/10.1016/j.stem.2015.02.015.
34. Cooper, J., and Giancotti, F.G. (2019). Integrin Signaling in Cancer: Mechanotransduction, Stemness, Epithelial Plasticity, and Therapeutic Resistance. Cancer Cell *35*, 347–367. https://doi.org/10.1016/j.ccell.2019.01.007.
35. Jahangiri, A., Aghi, M.K., and Carbonell, W.S. (2014). Beta1 integrin: Critical path to antiangiogenic therapy resistance and beyond. Cancer Res. *74*, 3–7. https://doi.org/10.1158/0008-5472.CAN-13-1742.
36. Hu, C., Ni, Z., Li, B.S., Yong, X., Yang, X., Zhang, J.W., Zhang, D., Qin, Y., Jie, M.M., Dong, H., et al. (2017). hTERT promotes the invasion of gastric cancer cells by enhancing FOXO3a ubiquitination and subsequent

ITGB1 upregulation. Gut *66*, 31–42. https://doi.org/10.1136/gutjnl-2015-309322.

37. Zhang, S., Zhao, B.S., Zhou, A., Lin, K., Zheng, S., Lu, Z., Chen, Y., Sulman, E.P., Xie, K., Bögler, O., et al. (2017). m^6A Demethylase ALKBH5 Maintains Tumorigenicity of Glioblastoma Stem-like Cells by Sustaining FOXM1 Expression and Cell Proliferation Program. Cancer Cell *31*, 591–606.e6. https://doi.org/10.1016/j.ccell.2017.02.013.
38. Zhang, N., Wei, P., Gong, A., Chiu, W.T., Lee, H.T., Colman, H., Huang, H., Xue, J., Liu, M., Wang, Y., et al. (2011). FoxM1 promotes beta-catenin nuclear localization and controls Wnt target-gene expression and glioma tumorigenesis. Cancer Cell *20*, 427–442. https://doi.org/10.1016/j.ccr.2011.08.016.
39. Lam, E.W.F., Brosens, J.J., Gomes, A.R., and Koo, C.Y. (2013). Forkhead box proteins: tuning forks for transcriptional harmony. Nat. Rev. Cancer *13*, 482–495. https://doi.org/10.1038/nrc3539.
40. Ling, S., Shan, Q., Zhan, Q., Ye, Q., Liu, P., Xu, S., He, X., Ma, J., Xiang, J., Jiang, G., et al. (2020). USP_{22} promotes hypoxia-induced hepatocellular carcinoma stemness by a $HIF1_{alpha}/USP_{22}$ positive feedback loop upon TP_{53} inactivation. Gut *69*, 1322–1334. https://doi.org/10.1136/gutjnl-2019-319616.
41. Sussman, R.T., Stanek, T.J., Esteso, P., Gearhart, J.D., Knudsen, K.E., and McMahon, S.B. (2013). The epigenetic modifier ubiquitin-specific protease 22 (USP22) regulates embryonic stem cell differentiation via transcriptional repression of sex-determining region Y-box 2 (SOX2). J. Biol. Chem. *288*, 24234–24246. https://doi.org/10.1074/jbc.M113.469783.
42. Cortez, J.T., Montauti, E., Shifrut, E., Gatchalian, J., Zhang, Y., Shaked, O., Xu, Y., Roth, T.L., Simeonov, D.R., Zhang, Y., et al. (2020). CRISPR screen in regulatory T cells reveals modulators of Foxp3. Nature *582*, 416–420. https://doi.org/10.1038/s41586-020-2246-4.
43. Huang, X., Zhang, Q., Lou, Y., Wang, J., Zhao, X., Wang, L., Zhang, X., Li, S., Zhao, Y., Chen, Q., et al. (2019). USP22 Deubiquitinates CD274 to Suppress Anticancer Immunity. Cancer Immunol. Res. *7*, 1580–1590. https://doi.org/10.1158/2326-6066.CIR-18-0910.
44. Gregory, S., Xu, Y., Xie, P., Fan, J., Gao, B., Mani, N., Iyer, R., Tang, A., Wei, J., Chaudhuri, S.M., et al. (2022). The ubiquitin-specific peptidase 22 is a deubiquitinase of CD73 in breast cancer cells. Am. J. Cancer Res. *12*, 5564–5575.
45. Li, J., Peng, L., Chen, Q., Ye, Z., Zhao, T., Hou, S., Gu, J., and Hang, Q. (2022). Integrin beta1 in Pancreatic Cancer: Expressions, Functions, and Clinical Implications. Cancers *14*, 3377. https://doi.org/10.3390/cancers14143377.
46. Alday-Parejo, B., Stupp, R., and Rüegg, C. (2019). Are Integrins Still Practicable Targets for Anti-Cancer Therapy? Cancers *11*, 978. https://doi.org/10.3390/cancers11070978.
47. Mezu-Ndubuisi, O.J., and Maheshwari, A. (2021). The role of integrins in inflammation and angiogenesis. Pediatr. Res. *89*, 1619–1626. https://doi.org/10.1038/s41390-020-01177-9.
48. Zeltz, C., Primac, I., Erusappan, P., Alam, J., Noel, A., and Gullberg, D. (2020). Cancer-associated fibroblasts in desmoplastic tumors: emerging role of integrins. Semin. Cancer Biol. *62*, 166–181. https://doi.org/10.1016/j.semcancer.2019.08.004.
49. Koivisto, L., Heino, J., Häkkinen, L., and Larjava, H. (1994). The size of the intracellular beta 1-integrin precursor pool regulates maturation of beta 1-integrin subunit and associated alpha-subunits. Biochem. J. *300*, 771–779. https://doi.org/10.1042/bj3000771.
50. Pang, X., He, X., Qiu, Z., Zhang, H., Xie, R., Liu, Z., Gu, Y., Zhao, N., Xiang, Q., and Cui, Y. (2023). Targeting integrin pathways: mechanisms and advances in therapy. Signal Transduct. Target. Ther. *8*, 1. https://doi.org/10.1038/s41392-022-01259-6.
51. Slack, R.J., Macdonald, S.J.F., Roper, J.A., Jenkins, R.G., and Hatley, R.J.D. (2022). Emerging therapeutic opportunities for integrin inhibitors. Nat. Rev. Drug Discov. *21*, 60–78. https://doi.org/10.1038/s41573-021-00284-4.
52. Raab-Westphal, S., Marshall, J.F., and Goodman, S.L. (2017). Integrins as Therapeutic Targets: Successes and Cancers. Cancers *9*, 110. https://doi.org/10.3390/cancers9090110.
53. Millard, M., Odde, S., and Neamati, N. (2011). Integrin Targeted Therapeutics. Theranostics *1*, 154–188. https://doi.org/10.7150/thno/v01p0154.
54. Shackleton, M., Vaillant, F., Simpson, K.J., Stingl, J., Smyth, G.K., Asselin-Labat, M.L., Wu, L., Lindeman, G.J., and Visvader, J.E. (2006). Generation of a functional mammary gland from a single stem cell. Nature *439*, 84–88. https://doi.org/10.1038/nature04372.
55. Hu, Y., and Smyth, G.K. (2009). ELDA: extreme limiting dilution analysis for comparing depleted and enriched populations in stem cell and other assays. J. Immunol. Methods *347*, 70–78. https://doi.org/10.1016/j.jim.2009.06.008.
56. Zhang, J., Lee, S.-M., Shannon, S., Gao, B., Chen, W., Chen, A., Divekar, R., McBurney, M.W., Braley-Mullen, H., Zaghouani, H., and Fang, D. (2009). The type III histone deacetylase Sirt1 is essential for maintenance of T cell tolerance in mice. J. Clin. Invest. *119*, 3048–3058. https://doi.org/10.1172/JCI38902.
57. Lin, Z., Yang, H., Kong, Q., Li, J., Lee, S.M., Gao, B., Dong, H., Wei, J., Song, J., Zhang, D.D., and Fang, D. (2012). USP22 antagonizes p53 transcriptional activation by deubiquitinating Sirt1 to suppress cell apoptosis and is required for mouse embryonic development. Mol. Cell *46*, 484–494. https://doi.org/10.1016/j.molcel.2012.03.024.
58. McCarty, K.S., Jr., Szabo, E., Flowers, J.L., Cox, E.B., Leight, G.S., Miller, L., Konrath, J., Soper, J.T., Budwit, D.A., Creasman, W.T., et al. (1986). Use of a monoclonal anti-estrogen receptor antibody in the immunohistochemical evaluation of human tumors. Cancer Res. *46*, 4244s–4248s.

STAR★METHODS

KEY RESOURCES TABLE

REAGENT or RESOURCE	SOURCE	IDENTIFIER
Antibodies		
Rabbit Anti-USP22	Abcam	Cat#ab195289; RRID: AB_2801585
Rabbit Anti-integrin β1	Proteintech	Cat#12594-1-AP; RRID: AB_2130085
Rabbit Anti-integrin β1	CST	Cat#34971T; RRID: AB_2799067
Mouse Anti-FoxM1	Santa Cruz	Cat#sc-376471; RRID: AB_11150135
Rabbit Anti-FoxM1	Abcam	Cat#ab207298; RRID: AB_3068347
Rabbit Anti-GAPDH	Proteintech	Cat#10494-1-AP; RRID: AB_2263076
Mouse Anti-Myc	Santa Cruz	Cat#sc-40; RRID: AB_2892598
Mouse Anti-Myc HRP	CST	Cat#2040s; RRID: AB_2148465
Rabbit Anti-GFP	CST	Cat#2956s; RRID: AB_1196615
Mouse Anti-Flag	Sigma	Cat#1804; RRID: AB_262044
Mouse Anti- Flag-HRP	Sigma	Cat#A8592; RRID: AB_439702
Mouse Anti-UB	CST	Cat#3936s; RRID: AB_331292
Mouse Anti-HA HRP	Santa cruz	Cat#sc-7392; RRID: AB_627809
Anti-APC-integrin α1	Biolegend	Cat#142605; RRID: AB_2562252
Anti-APC-integrin α2	Invitrogen	Cat#17-5971-81; RRID: AB_469484
Anti-APC-integrin α3	R&D	Cat#FAB2787A; RRID: AB_1538109
Anti-FITC-integrin α4	Biolegend	Cat#103605; RRID: AB_313036
Anti- FITC-integrin α5	Invitrogen	Cat#11-0493-81; RRID: AB_1234968
Anti-FITC-integrin α6	Invitrogen	Cat#11-0495-82; RRID: AB_11150059
Anti-APC-integrin α7	Thermo	Cat#MA5-23555; RRID: AB_2607368
Anti-PE-integrin α8	Thermo	Cat#MA5-23677; RRID: AB_2608542
Anti-APC-integrin β1	Invitrogen	Cat#17-0291-82; RRID: AB_1210793
Anti-PE-integrin β2	BD	Cat#553293; RRID: AB_394762
Anti-PE-integrin β3	BioLegend	Cat#104307; RRID: AB_313084
Anti-PE-integrin β4	BioLegend	Cat#123609; RRID: AB_2563543
Anti-FITC-integrin β5	eBioscience	Cat#11-0497-42; RRID: AB_10547284
Anti-APC-integrin β6	Miltenyi	Cat#130-111-454; RRID: AB_2652496
Anti-APC-integrin β7	BioLegend	Cat#321207; RRID: AB_571964
Anti-APC-integrin β8	Biorbyt	Cat#orb488142
Anti-PE-CD44	eBioscience	Cat#12-0441-82; RRID: AB_465664
Anti-FITC-CD44	Abcam	Cat#11-0441-81; RRID: AB_465044
Anti-APC-CD24	BioLegend	Cat#101814; RRID: AB_439716
Oligonucleotides		
Mouse *β-actin* (forward): AGATCAAGATCATTGCTCCTCCT	IDT	
Mouse *β-actin*_(reverse): ACGCAGCTCAGTAACAGTCC	IDT	
Mouse *FoxM1*_(forward): CAGAATGCCCCGAGTGAAACA	IDT	
Mouse *FoxM1*_(reverse): GTGGGGTGGTTGATAATCTTGAT	IDT	
Mouse *CD44*_(forward): TCTGCCATCTAGCACTAAGAGC	IDT	
Mouse *CD44*_(reverse): GTCTGGGTATTGAAAGGTGTAGC	IDT	
Mouse *ITGB1*_(forward): ATGCCAAATCTTGCGGAGAAT	IDT	
Mouse *ITGB1*_(reverse): TTTGCTGCGATTGGTGACATT	IDT	

(*Continued on next page*)

Continued

REAGENT or RESOURCE	SOURCE	IDENTIFIER
Mouse *ALDH*_(forward): GGGTGGGCAGACAAAATCCA	IDT	
Mouse *ALDH*_(reverse): AGAGGCTAGGTACAGAGCCG	IDT	
Mouse *Nanog*_(forward): TCGCCCTTCCTCTGAAGAC	IDT	
Mouse *Nanog*_(reverse): TGCTTCTGAAACCTGTCCTTGA	IDT	
Mouse *USP22*_(forward): CTCCCCACACATTCCATACAAG	IDT	
Mouse *USP22*_(reverse): TGGAGCCCACCCGTAAAGA	IDT	
Human *β-actin* (forward): AAGTGTGACGTGGACATCCGC	IDT	
Human *β-actin* (reverse): CCGGACTCGTCATACTCCTGCT	IDT	
Human *FoxM1*_(forward): CGTCGGCCACTGATTCTCAAA	IDT	
Human *FoxM1*_(reverse): GGCAGGGGATCTCTTAGGTTC	IDT	
Human *CD44*_(forward): CTGCCGCTTTGCAGGTGTA	IDT	
Human *CD44*_(reverse): CATTGTGGGCAAGGTGCTATT	IDT	
Human *ITGB1*_(forward): CCTACTTCTGCACGATGTGATG	IDT	
Human *ITGB1*_(reverse): CCTTTGCTACGGTTGGTTACATT	IDT	
Human *ALDH*_(forward): TGAATGGCACGAATCCAAGAG	IDT	
Human *ALDH*_(reverse): CACGTCGGGCTTATCTCCT	IDT	
Human *Nanog*_(forward): TTTGTGGGCCTGAAGAAAACT	IDT	
Human *Nanog*_(reverse): AGGGCTGTCCTGAATAAGCAG	IDT	
Human USP22_(forward): CCATTGATCTGATGTACGGAGG	IDT	
Human *USP22*_(reverse): TCCTTGGCGATTATTTCCATGTC	IDT	
Oligo sequences of sgRNAs of USP22 (5′-3′)		
Human sgRNA target USP22: GCCATTGATCTGATGTACGG	IDT	
Mouse sgRNA target USP22: GCCATCGACCTGATGTACGG	IDT	

RESOURCE AVAILABILITY

Lead contact

Further information and requests for resources and reagents should be addressed to and will be fulfilled by the lead contact (fangd@northwestern.edu).

Materials availability

This study did not generate new reagents. All materials in this study are commercially available. Plasmids and associated vector maps generated is this study are available upon request to the lead contact.

Data and code availability

- Data from publicly archive datasets are available from cBiolPortal database for breast cancer cell RNA-Seq data. Any additional information requires to reanalyze the data reported in this paper is available from the lead contact upon request.
- The data are available to academic researchers from corresponding author upon reasonable request.

EXPERIMENTAL MODEL AND STUDY PARTICIPANT DETAILS

Human breast cancer tissue microarray

Human breast cancer tissue microarrays were commercially available from Shanghai Outdo Biotech Co., Ltd.

METHOD DETAILS

Cell culture

Human HEK-293T cells were cultured in DMEM medium plus 10% FBS (Thermo Fisher Scientific,10437028) and 1% penicillin and streptomycin. 4T1 cells were maintained in RPMI medium supplemented with 10% FBS and 1% penicillin and streptomycin. TN1 cells were cultured in HuMEC-ready medium (Life Technologies) supplemented with 5% FBS and 0.5% P/S in collagen type I (BD Biosciences) coated plates.

Molecular cloning and plasmid

The full length USP22 cDNA (NM_001004143.4) was amplified by PCR and subcloned into pEGFP-C1 (NovoPro Bioscience: Cat#V012024) plasmid to construct GFP-USP22 fusion protein. The pEGFP-C1-GFP-USP22 plasmid was transfected into 4T1-USP22 depleted cells. Cells were treated with 200 μg/mL of neomycin for 4 days followed by sorting of GFP positive cells. For the rescue experiments, full length *FOXM1* (NM_008021) and *ITGB1* (NM_010578.2) cDNA were amplified by PCR and constructed into the pLV-EF1a-IRES-Blast (Addgene, Cat#85133). The lentiviral vector was co-transfected with the packaging vector (psPAX2 and pMD2.G) into HEK-293T cells by jetOPTIMUS transfection reagent (Cat#101000006) to generate lentiviruses. The lentiviruses were collected and filtered by 0.45 μm filter after 48 h transfection. Indicated cells were infected with the lentivirus in the presence of 8 μg/mL polybrene. The positive cells were then selected by treatment with 4 μg/mL blasticidin for four days to establish stable cells expressing either FoxM1 or integrin β1. The truncation of $USP22^{1-160}$ and $USP22^{161-525}$ were amplified by PCR and a stop codon or a start codon were introduced, respectively, and then subcloned into pCMV-Myc (Addgene: Cat#2223) plasmid. Human or mouse USP22 single guide RNA sequence was ligated into lentiCRISPR v2 (Addgene: Cat#52961) plasmid separately. Indicated cells were transiently transfected. 48 h after transfection, cells were selected using 2 μg/mL puromycin for 4 days. The efficacy of USP22 deletion was validated by western blotting. The sequences of each guide RNA used in this study are listed in key resources table.

Tumor sphere formation assay

A total of 3×10^4 4T1 or TN1 cells with or without USP22 sgRNA were plated into ultralow-attachment 6-well plates (Corning, Cat#3471), and maintained in EpiCult-B Basal Medium (Human) (Stem Cell Technologies, BC, Canada) and EpiCult-B Proliferation Supplement (Human) (Stem Cell Technologies, BC, Canada), and supplemented with 2 U/mL heparin and 0.5 mg/mL hydrocortisone (Sigma H0135). LLC1 and MC38 cells were cultured in serum-free DMEM/F12, supplemented with B27 (Invitrogen, 2175161), 20 ng/mL EGF, 20 ng/mL and 1% penicillin/streptomycin. After 10 days of culture, the spheres were pictured, and the number of spheres in each group were counted.

Colony formation assay

A total of 300 indicated cells were seeded into 35 mm dishes in triplicate and maintained in culture for two weeks. The culture medium was changed every 3 days. When colonies grew to visible size, the colonies were then washed twice with phosphate buffered saline and fixed with 4% formaldehyde for 30 min at room temperature and stained for 1 h with 0.1% crystal violet. After staining, the plates were gently washed with distilled water and air-dried. The exact colony number of colonies was then quantified by ImageJ software.

Cell viability

A total of 10^4 indicated cells were seeded into 96 well plate. 12h later, cells were treated with S02 at the designated concentration for 24 h. Following this, Cells were fixed with 10% trichloroacetic acid (Sigma, T6399) for 1 h at 4°C. The wells were gently washed with distilled water and allowed to air-dry and subsequently subjected to stain with 1% SRB (Sigma, S9012) for 10 min at room temperature. After washing with 1% acetic acid (Sigma, 695092), bound SRB was then solubilized with 50 μL Tris buffer (10 mM), and the OD_{515} values were evaluated by spectrometer.

In vitro extreme limiting dilution assay

Indicated cells were dissociated into single cell suspensions and seeded into 96-well plates at densities of 5, 10, 15, 20 cells per well using previously mentioned tumor sphere formation medium. Cells were incubated at 37°C for 10 to 14 days. At the time of quantification, each well was counted for formed tumor spheres. Stem cell frequency was calculated using extreme limiting dilution analysis online tool[55] (http://bioinf.wehi.edu.au/software/elda/).

Real-time PCR

Total RNA was extracted from indicated cells using Trizol. The cDNA was synthesized using a Quantifect Reverse Transcription Kit. qRT-PCR was performed using SYBR Premix Ex Taq, primers, H_2O, and cDNA (final reaction volume, 20 mL). The sequences of the primers used in this study are listed in key resources table.

Flow cytometry analysis and cell sorting

Prior to $CD24^-/CD44^+$ BCSCs sorting, 4T1 and TN1 cells were washed with PBS, dissociated using accutase, counted and incubated with primary antibody against CD44 and CD24 on ice for 60 min. FacsAria (BD) cell sorter was used to isolate $CD24^-/CD44^+$ and $CD24^+/CD44^-$ cells, respectively. For the 4T1 GFP-USP22 fusion knock-in cells, cells were dissociated using accutase. Cells were then sorted using FacsAria (BD) cell sorter based on fluorescence intensity. For integrin family expression evaluation, indicated cells were dissociated using accutase followed by staining with indicated antibodies on ice for 60 min. Cells were run on the BD-LSR Fortessa X-20 (BD Biosciences) instrument and flow analyses were done using FlowJo software. Antibodies used for flow cytometry are listed in key resources table.

Immunoblot

Indicated cells in this study were lysed with RIPA buffer supplemented with protease inhibitors. The same quantity of protein was subjected to SDS-PAGE gel electrophoresis, transferred onto polyvinylidene fluoride membranes, and blocked with 5% skimmed milk for 30 min at room temperature. The membranes were then incubated with primary antibodies. The detailed information of antibodies used in this study are listed in key resources table.

Co-immunoprecipitation

TN1 or 4T1 cells were harvested and lysed with RIPA buffer containing protease inhibitors. Cell lysates were precleared using protein A/G beads (10294276, GE healthcare) for 1 h on a shaker at 4°C. Protein A/G beads were then removed, and primary antibody added followed by overnight incubation on a shaker at 4°C. New protein A/G beads were subsequently added for another 2 h incubation. Beads were then collected following washing with ice-cold PBS for 4 times. The precipitate was washed by RIPA buffer for five times. After each wash, the precipitate was gently shaking for 5 min. Finally, the bound protein was eluted by boiling for 5 min and subjected to SDS-PAGE.

Chromatin immunoprecipitation (Ch-IP) qPCR

A total of 5×10^6 4T1 USP22 ablation or control cells were cross-linked with 1% formaldehyde for 10 min at 37°C, washed with PBS, and suspended in SDS-lysis buffer (50 mM Tris-HCl, 1% SDS, 10 mM EDTA, pH 8.1). The lysate was treated with RNase and then sonicated. After centrifugation, supernatants were subjected to immunoprecipitation with primary FoxM1 antibodies. The enrichment of FoxM1 consensus site (C/TAAAC/TA) in *ITGB1* promoter sequences was detected by quantitative PCR using gene-specific primers and SYBRGreen (Applied Biosystems).

Dual-luciferase assay

ITGB1 promoter sequences (−2000 to TSS) were inserted into upstream of the *Firefly luciferase gene* in a pGL4 vector. 4T1 USP22 depletion or control cells were seeded into 12-well plates and transfected with pGL3 luciferase vector containing with the promoter of *ITGB1*. Transfection efficiency was quantified by co-transfection with Renilla luciferase reporter. The activities of firefly luciferase and Renilla luciferase in each well were evaluated by a dual-luciferase reporter assay system kit (Promega, E1910). The ratios between the luciferase reporter and Renilla control were determined 48 h after transfection.

Immunohistochemistry

Immunohistochemical (IHC) staining was performed following the standard protocol as reported.[56,57] Briefly, tissue specimens were subjected to deparaffinization in xylene, rehydrated through graded ethanol solutions, followed by antigen retrieval, and immersed in a 0.3% hydrogen peroxide solution. Slides were washed three times with phosphate-buffered saline (PBS), and nonspecific antigens were blocked by incubation with 5% bovine serum albumin for 30 min at room temperature. The tissue slides were subsequently incubated with primary antibodies overnight at 4°C. Horseradish peroxidase (HRP) conjugated secondary antibody was used to incubate the slides before DAB detection. For the IHC results analysis, the percentage score was assigned as follows: 1 indicated that 0–25% of the tumor cells showed a positive signal, 2 indicated 26–50% of cells were stained, 3 indicated 51–75% stained, and 4 indicated 76–100% stained. We scored the staining intensity as 0 for negative, 1 for weak, 2 for moderate, and 3 for strong. The total score was obtained by multiplying the percentage score by the stain intensity score. Antibodies used for IHC are listed in key resources table.

Tissue microarray

Breast cancer tissues with fully annotated clinical and pathological information were obtained from Shanghai Outdo Biotech Co., Ltd. The Immunohistochemical staining was performed as described as immunohistochemistry. Histoscore (H score) was unbiasedly calculated by the company using a semi-quantitative approach according to standard protocol.[58] Briefly, histochemical scoring (H-score) assessment incorporating both the staining intensity (i) and a percentage of stained cells at each intensity level (Pi). The i values are graded as: 0, non-staining; 1, weak; 2, median; or 3, strong. The Pi values vary from 0% to 100%. The final H-score is derived from the sum of i multiplied by Pi as the equation H score= $(0X\ P_0) + (1XP_1) + (2XP_2) + (3XP_3)$.

Animal studies

All animal experiments were approved by the Institutional Animal Care and Use Committee at Northwestern University. All mice were maintained in a specific pathogen-free facility. BALB/c, and NSG mice at the age of 6–8 weeks were all purchased from Jackson laboratory. For the metastatic mice model, BALB/c mice were intravenously administrated with 5×10^4 4T1 USP22 ablation or control cells. 20 days later, all the mice were sacrificed and analyzed for the presence of metastatic nodules. For the mice survival analysis, BALB/c mice were intravenously administrated with 5×10^4 4T1 wildtype cells. Mice were euthanized until they exhibited signs of significantly declining quality of life (e.g., ataxia, lethargy, seizures, inability to feed) and the survival of mice were recorded. For the S02 treatment, BALB/c mice were intravenously administrated with 5×10^4 4T1 cells. 24 h later, mice were randomized into treatment groups and treated with S02 (10 mg/kg), or vehicle control by intraperitoneal injection six times (once every day). Mice were sacrificed 3 weeks later after 4T1 cells administration, and the lung of

mice were taken out to analyze tumor nodules. For the orthotopic xenograft model, 5×10^4 TN1 cells were orthotopically injected into the mammary fat pad of NSG mice, 2 weeks later, mice were randomized into treatment groups and treated with S02 (20 mg/kg), or vehicle control group by intraperitoneal injection six times (twice every day).

QUANTIFICATION AND STATISTICAL ANALYSIS

Data are represented as the mean ± SD, and error bars indicate SD. *p* values were calculated by either unpaired or paired two-tailed Student's t test, $*p < 0.05$, $**p < 0.01$, and $***p < 0.001$. All analyses were performed using GraphPad Prism software (GraphPad Software, Inc.).